MASTER OF PHILOSOPHY

Vascular changes in Alzheimer's disease and other types of dementia in the retina of human and animal

Hunter, Leanne

Award date:
2017

Awarding institution:
Queen's University Belfast

Vascular Changes in Alzheimer's Disease and Other Types of Dementia in the Retina of Human and Animal

Leanne Hunter

40104615

MRes Translational Medicine

Supervisor: Dr Imre Lengyel

Faculty: School of Medicine, Dentistry & Biomedical Sciences

Degrees held: BSc Biomedical Science

Date: 18/09/17

Word Count: 15,255

Abstract

Alzheimer's disease is a complex condition which manifests within the brain causing loss of brain function and resultant cognitive decline. The retina is closely related to the brain and it has been proposed that the retina may be adversely affected in Alzheimer's disease (AD). If AD-associated pathologies can be detected in the retina and they correlate with brain pathology, this has the potential to solve clinical problems regarding the diagnosis and monitoring of AD. Recent research has shown that amyloid beta (Aβ); the protein responsible for cerebral amyloid plaques in AD may also accumulate within the retina in those affected by the condition. My research involved the application of immunohistochemistry techniques to identify Aβ within the retina of AD individuals and transgenic mouse models of AD, and to explore if an association exists between Aβ and retinal vasculature. Aβ accumulations were identified in flat-mount retina and cross-sections from AD and age-matched control eyes. Aβ labelling was found in clusters associated with retinal blood vessels, in spherical structures within drusen, choroid and sclera and an intracellular labelling was detected in the inner layers of the human retina. Where Aβ accumulations were detected extracellularly in the human retina, these were in few areas. No increase in Aβ accumulations was seen in the retina of AD samples when compared to age-matched controls. No Aβ accumulations were found in the retinas of transgenic mouse models of AD but an intracellular labelling was detected in the inner retina, similar to findings in human tissue. Based on these findings, it is not possible to conclude that retinal Aβ deposits have the potential to reflect the hallmark cerebral Aβ plaques which contribute to the progression of AD. Given the challenges associated with the diagnosis and treatment of AD, the concept of abnormal retinal Aβ accumulation as a potential pathology of AD should not be overlooked until further in-depth research has been carried out.

Introduction

Alzheimer's disease (AD) is a progressive, neurodegenerative condition which primarily affects the brain and can lead to severe cognitive impairment. It is the most common subtype of dementia affecting approximately 46.8 million people worldwide (Prince et al., 2016). Dementia is the set of symptoms resulting from cognitive decline such as language and behavioural problems, memory loss and confusion. With progression of AD, the symptoms worsen and begin to interfere with daily life. At present, the pathogenesis of AD is not coherently understood therefore no curative therapies for the condition have been developed.

Alzheimer's Disease – Amyloid beta and Tau

AD is characterised by neurodegeneration within the brain. The neurodegenerative process is thought to involve neuronal loss (Yankner et al., 1996; Padurariu et al., 2012), synaptic changes (Selkoe, 2002; Scheff et al., 2006), inflammatory mechanisms (Akiyama et al., 2000; Frautschy et al., 1998) and oxidative stress (Christen, 2000; Manczak et al., 2006). This vast cerebral degeneration results in shrinkage of the brain when compared to that of a healthy individual (Double et al., 1996). Although the exact pathogenesis of the condition is not clearly defined, it has been linked to abnormal accumulations of misfolded proteins within the brain. The two main proteins associated with AD are amyloid beta (Aβ) and tau. Aβ and tau are present in the healthy brain; however, are abnormally processed and accumulate in AD leading to the hallmark brain pathologies; senile plaques consisting of Aβ (Masters et al., 1985) and neurofibrillary tangles (NFTs) consisting of hyperphosphorylated tau (Grundke-Iqbal et al., 1986) (Figure 1). The mechanisms in which these two abnormal protein accumulations lead to neurodegeneration remain incompletely understood.

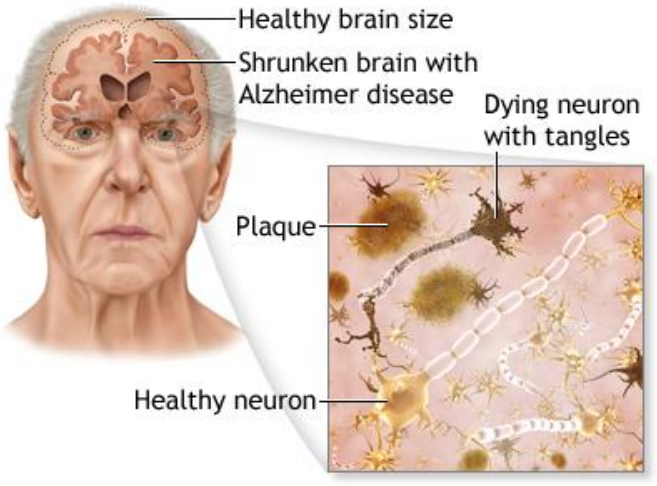

Figure 1. **Alzheimer's Disease.** Extracellular amyloid plaques and intracellular neurofibrillary tangles of tau protein are thought to induce cerebral tissue damage and result in shrinkage of the brain (A.D.A.M, 2017).

Cerebral plaques consisting of Aβ are one of the two hallmark lesions described in AD. The formation of these extracellular plaques involves processing of the membrane-bound amyloid precursor protein (APP) (Figure 2). APP can be processed via two pathways; amyloidogenic and non-amyloidogenic. The amyloidogenic pathway results in the formation of Aβ peptides. In this pathway, APP is sequentially cleaved by β-secretase to generate sAPPβ and C99 fragments. C99 is then cleaved by γ-secretase to generate Aβ peptides. This cleavage by γ-secretase can generate Aβ peptides of various lengths, of which 40 amino acids (Aβ40) and 42 amino acids (Aβ42) are the most frequently formed (Selkoe, 2001). APP can also be processed via the non-amyloidogenic pathway which does not generate Aβ peptides. In this case, APP cleavage by α-secretase results in the fragments sAPPα and C83. C83 can then be cleaved by γ-secretase to form AICD and p3 fragments.

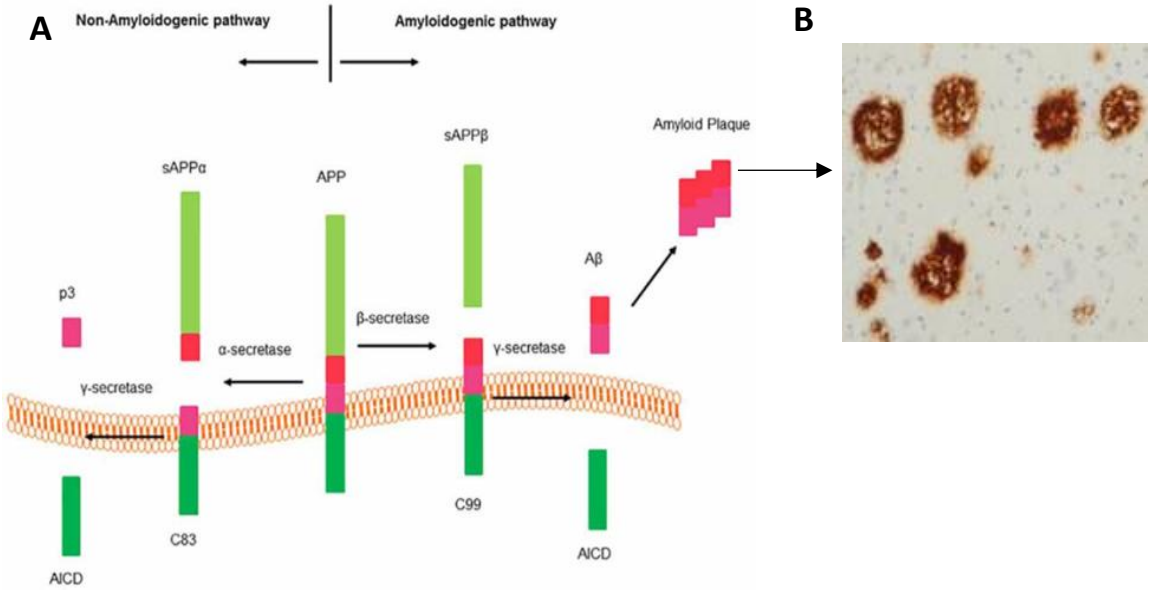

Figure 2. **Processing of amyloid precursor protein (APP) and amyloid plaque formation.** (A) APP can be processed via amyloidogenic or non-amyloidogenic pathways. Amyloidogenic involves APP cleavage by β-secretase to form sAPPβ and C99. Membrane bound C99 is then cleaved by γ-secretase to form Aβ peptides which can aggregate into Aβ plaques. Non-amyloidogenic processing involves sequential cleavage by α-secretase and γ-secretase to generate p3 and AICD fragments. No Aβ peptides are formed via this pathway. (B) Cerebral Aβ plaques (Zhao et al., 2016; Serrano-Pozo et al., 2011).

The most frequently formed Aβ peptides are Aβ40 and Aβ42. The longer peptide Aβ42 is more prone to aggregation and is overproduced in individuals which suffer from AD. Aβ42 is the most abundant form in cerebral plaques; however, Aβ40 can also be aggregated (Hardy & Selkoe, 2002).

NFTs consisting of hyperphosphorylated tau are another neuropathology characterised in the AD brain. Tau is a protein which facilitates microtubule stability within cells. It can become increasingly phosphorylated by kinases, hyperphosphorylated tau aggregates together and is sequestered into intracellular NFTs (Figure 3). This leaves less tau available for microtubule stability leading to degeneration of neuronal cells (Selkoe, 2001).

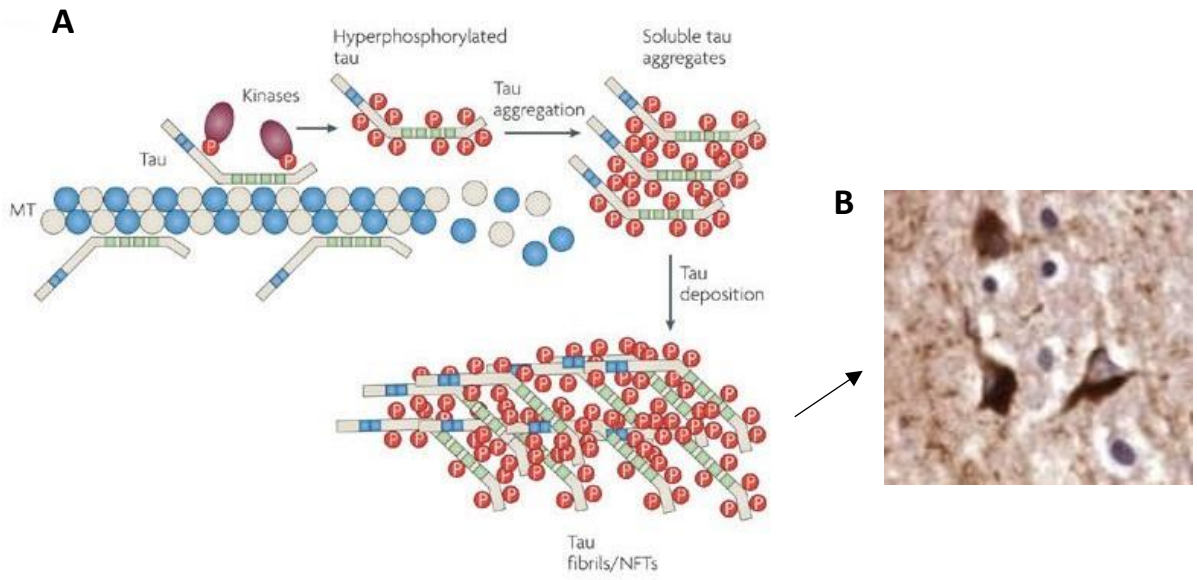

Figure 3. **Formation of neurofibrillary tangles (NFTs) of hyperphosphorylated tau.** (A) Microtubule (MT)-associated protein tau is phosphorylated by kinases. Hyperphosphorylated tau aggregates to form soluble aggregates which are deposited into NFTs. (B) NFTs within the brain (Götz & Ittner, 2008; Serrano-Pozo et al., 2011).

Amyloid and Vascular Hypotheses for AD

The exact initiating events responsible for the formation of Aβ plaques and NFTs and therefore the onset of AD are incompletely understood. One hypothesis which has been extensively studied is the amyloid cascade hypothesis (Hardy & Higgins, 1992). It suggests that the deposition of Aβ into extracellular senile plaques is the initiating event in the pathogenesis of AD and the presence of these plaques induces the formation of intracellular NFTs consisting of hyperphosphorylated tau

(Hardy & Higgins, 1992; Götz et al., 2001). All the other characteristics that accompany AD such as inflammation, vascular dysfunction and neuronal damage are also thought to result from these cerebral plaques (Hardy & Higgins, 1992). The overproduction of Aβ peptides which leads to their deposition is thought to be due to a disruption in the mechanisms responsible for production and clearance of the peptides (Hardy & Selkoe, 2002). However, it is unknown whether the neurodegenerative process relies on the formation of senile plaques or whether individual Aβ peptides can cause the neuronal damage associated with AD (Selkoe, 2001).

More recently a vascular hypothesis for AD onset has been explored (De La Torre, 2002; De La Torre, 2004). This hypothesis suggests that neurovascular dysfunction may be responsible for initiating AD. Cerebral vascular dysfunction can lead to a lack of brain perfusion and hence hypoxia. Consequently, neurones within the brain would not be adequately supplied with blood and neuronal cell death would occur (Zlokovic, 2011). This vascular-associated damage may induce the overexpression and aggregation of Aβ peptides and their deposition into cerebral plaques (Koike et al., 2010; Garcia-Alloza et al., 2011). Further evidence which proposes that AD may have a vascular disease component includes vascular risk factors such as diabetes mellitus, hypertension, heart disease and smoking which are associated with a reduction of cerebral perfusion and have been found to increase the risk of AD (Luchsinger et al., 2005). In addition, one of the key AD proteins has been found to be associated with cerebral vasculature. Cerebral amyloid angiopathy is a condition in which Aβ is deposited in the walls of cerebral blood vessels. This process may narrow blood vessels and hence affect cerebral blood supply. The condition is commonly found in AD and may contribute to its pathogenesis (Thal et al., 2008). Furthermore, dementia due to a lack of cerebral blood supply is clinically diagnosed as vascular dementia. Vascular dysfunction can co-exist with AD-associated pathologies (cerebral Aβ plaques and NFTs) which is termed mixed dementia. Therefore, an overlap exists between vascular dementia and AD which further supports that AD has a vascular basis (Iadecola, 2010). AD is a complex condition in which the exact causal mechanisms are not well established; however, collectively this evidence would strongly suggest that vascular involvement contributes to the pathogenesis of AD.

Clinical Challenges in the Diagnosis and Monitoring of AD

The uncertainty surrounding the mechanisms responsible for AD onset and progression has led to a number of clinical challenges (Tarawneh & Holtzman, 2012). Difficulties have arisen in the diagnosis and monitoring of the condition. Making an early diagnosis of AD is almost impossible as a definitive diagnosis can only be established by identification of cerebral Aβ plaques and NFTs during post-mortem examination of the brain. Individuals can be diagnosed with possible or probable AD based on their clinical symptoms; however, this will not be confirmed until after death (McKhann et al., 2011). Current methods for diagnosis and monitoring include brain imaging scans such as positron emission tomography (PET), computed tomography (CT) and magnetic resonance imaging (MRI). Although brain scans are not ideal as they are expensive, not widely available to the vast amount of suspected AD sufferers and unable to diagnose the condition with complete certainty (Johnson et al., 2012). Cerebral spinal fluid (Ferreira et al., 2014) or blood samples (Koyama et al., 2012) may be analysed in an attempt to locate biomarkers such as Aβ or phosphorylated tau (ptau); however, this involves invasive procedures and results are not reliable enough to be used in routine diagnosis of AD. Furthermore, a major concern is that current diagnostic methods focus mainly on the elimination of other conditions and none are reliable enough to diagnose AD with complete certainty. A highly specific & sensitive diagnostic method for AD has yet to be established. As well as these, the abnormal protein accumulations of Aβ plaques and NFTs in the brain have been described to manifest years before symptoms of cognitive decline appear in sufferers (Price et al., 2009). This makes it impossible to make an early diagnosis in the presymptomatic stages of AD. Methods which can identify AD-associated pathologies early in the disease progression are urgently needed. First, a better understanding of the pathogenesis of the condition is required in order to provide patients with a more accurate and earlier diagnosis. Cerebral plaques and NFTs which present within the brain in AD makes them ideal targets for AD diagnosis; however, effective strategies to locate these early in disease progression have not yet been developed. The condition currently has no curative therapies and treatment options available can only alleviate the symptoms and slow the progression of AD. A greater understanding of the disease mechanisms needs to be established to allow an earlier detection and improve the therapeutic options available for AD.

Could Retinal Pathology Represent Brain Pathology in AD?

AD is a condition which predominantly affects the brain. The eye has been described as the 'window to the brain' and recent research has proposed that the retina may too be adversely affected in AD (Lim et al., 2016; Javaid et al., 2016). The retina is a light-sensitive tissue located at the back of the eye. Its function is to convert light rays into neural signals which are relayed to the brain via the optic nerve. The retina is directly linked to the brain, both are part of the central nervous system and have common embryonic origin, evolving from the neural crest (Etchevers et al., 2001). Given that the retina is a developmental outgrowth of the brain, it is not surprising that AD pathologies may develop in the eye. As a result, the identification of AD-associated changes within the retina is a growing area of research. Retinal abnormalities which may be associated with AD include the degeneration of retinal ganglion cells (Blanks et al., 1996), nerve fibre layer thinning (Berisha et al., 2007), optic nerve degeneration (La Morgia et al., 2016), reductions in blood flow (Berisha et al., 2007), vasculature changes (Frost et al., 2013; Williams et al. 2015), Aβ and ptau accumulation (Koronyo-Hamaoui et al., 2011; La Morgia et al., 2016; Koronyo et al., 2017; Schön et al., 2012) and inflammation (Liu et al., 2009). The retina is a tissue which can be easily accessed, viewed non-invasively and inexpensively making it an ideal target for in vivo imaging of AD. If retinal pathology is representative of brain pathology in AD, investigation of the retina could potentially provide an answer to the clinical problems regarding the condition.

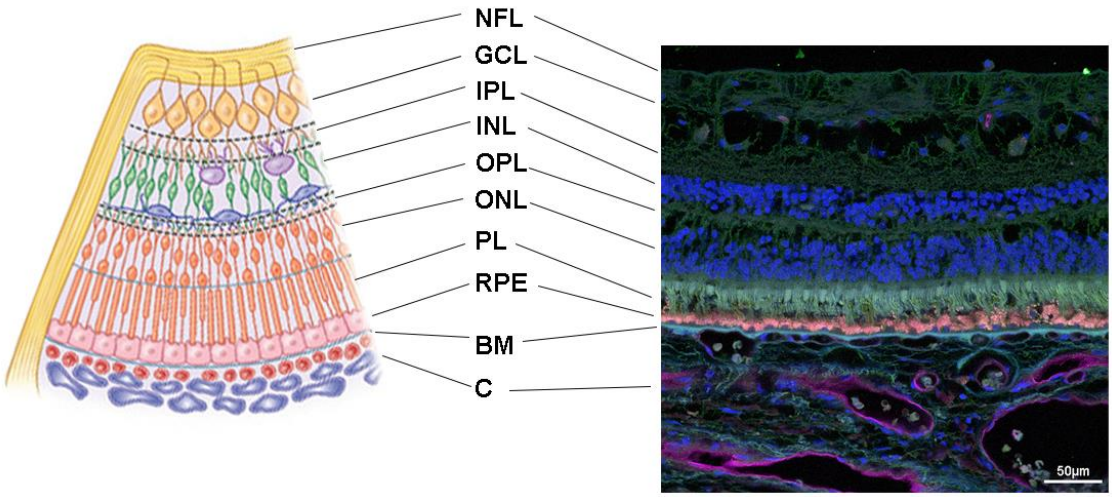

Figure 4. **Structure of the retina.** Retinal layers can be seen in the diagram (left) and confocal microscopic image (right). NFL-nerve fiber layer, GCL-ganglion cell layer, IPL-inner plexiform layer, INL-inner nuclear layer, OPL-outer plexiform layer, ONL-outer nuclear layer, PL-photoreceptor layer, RPE-retinal pigment epithelium, BM-Bruch's membrane and C-choroid (The Retina Reference, 2017).

Evidence of Retinal Aβ Deposits in AD

The presence of abnormal accumulations of Aβ in the AD retina remains controversial. My research has focused mainly on the identification of Aβ deposition within the AD retina by immunohistochemistry techniques. Research in animal models of AD has produced promising results; however, few experimental studies have successfully managed to identify Aβ deposits within the retina in human AD patients. The main research studies investigating Aβ deposition within the retina of human and animal and the methods used will be briefly described.

Firstly in terms of human retinal Aβ deposition, a key experimental study of interest conducted by Koronyo-Hamaoui et al. (2011) claimed to identify Aβ plaques within the retina of human post-mortem eyes using a variety of different anti-Aβ antibodies as well as curcumin, a dye which binds to Aβ. They analysed 8 definite AD and 5 possible/probable AD retinas. Plaques were mainly found in the inner layers of the retina and different plaque morphologies were identified. A study by La Morgia et al. (2016) which included some of the same investigators as the previous study, managed to identify retinal Aβ plaques when investigating 5 post-mortem AD patient's eyes using anti-Aβ monoclonal antibodies. They also detected an Aβ plaque in a healthy control retina. Similarly, a small study detected Aβ plaque-like structures in whole-mount retinas from 2 AD sufferers using the anti-Aβ antibody 6E10, the location within the retina was not specified (Tsai et al., 2014). Use of the 6E10 antibody will be highlighted in various studies as this is the anti-Aβ antibody predominantly used for the detection of Aβ in my research. A recent study conducted by Koronyo et al. (2017) which again included some of the same investigators as the initial study described, detected Aβ deposits within the retinas of 23 AD post-mortem eyes. An increase in retinal Aβ deposits were found in AD samples when compared to healthy age-matched controls. Retinal deposits were mainly found in the inner retinal layers and correlated with brain pathology of both AD and age-matched control samples. Classical, compact and diffuse plaques were identified and showed similar morphology but were smaller in size than cerebral plaques. Samples were analysed using a variety of antibodies specific to different regions of the Aβ peptide including the 6E10 antibody, and dyes which label Aβ. A loss of neuronal cells was also apparent in AD retinas when compared to healthy age-matched controls. Following on from in vivo imaging in live transgenic mice in a previous study (Koronyo-Hamaoui et al., 2011), the present study demonstrated in vivo detection of Aβ deposits in 10 live AD patients. Patients were administered with curcumin and retinas were visualised with a scanning laser ophthalmoscope. Numerous individual plaques and

clusters of Aβ deposits were identified in the retinas of AD patient's whist sparse deposits were located in age-matched controls.

Conversely, some researchers report a lack of Aβ deposition in the retina of AD patients. Schön et al. (2012) failed to detect any Aβ plaques when investigating 6 human AD post-mortem retinas using an anti-Aβ monoclonal antibody. Another study reported similar findings, failing to detect Aβ plaques in the 11 human AD post-mortem retinas analysed with an anti-Aβ monoclonal antibody and concluded that Aβ does not accumulate in the retina in an analogous state to within the brain (Ho et al., 2014).

Aside from the retina, Aβ has been detected in other areas of the human eye. Goldstein et al. (2003) managed to detect Aβ40 & Aβ42 in the lens of non-AD and AD eyes and Aβ40 in aqueous humour of non-AD eyes. A variety of different techniques were used which included immunohistochemistry, mass spectrometry, western blot, and slit-lamp stereophotomicroscopy. They concluded that concentrations of Aβ in the lens and aqueous humour were comparable to those within the AD brain and cerebral spinal fluid respectively. Aggregates of Aβ have been detected in sub-retinal pigment epithelium (sub-RPE) structures known as drusen. Drusen are extracellular deposits which are located between the Bruch's membrane and RPE. They can occur normally throughout the aging process (Löffler et al., 1995) but are also a pathogenic characteristic of age-related macular degeneration (AMD) (Anderson et al., 2004). Drusen are known to contain a diverse array of components such as Aβ, hydroxyapatite (HAP) and inflammatory and complement components (Anderson et al., 2004; Thompson et al., 2015; Mullins et al., 2000; Johnson et al., 2000). Aβ peptides aggregate within drusen and present in a spherical form (Anderson et al., 2004; Johnson et al., 2002). The ability for Aβ to spontaneously aggregate within drusen and AD-associated cerebral plaques may suggest similarities between drusen deposition and AD (Ritchie et al., 2011).

With the difficulties associated with human tissue in research, animal models are being increasingly used to investigate AD. Transgenic animal models of AD focus mainly on the amyloid hypothesis and replicate elevated levels of Aβ by overexpressing APP and presenilins; which are members of the γ-secretase complex. This elevated level of Aβ results in its deposition into cerebral Aβ plaques which are characteristic in the AD brain. Research into whether Aβ accumulates in the retina of transgenic animal models of AD has resulted in more conclusive findings than research into human retinal tissue. Aβ plaques have been identified in the retina of animal models of AD by various experimental studies. The same study as previously

mentioned by Koronyo-Hamaoui et al. (2011) investigated the $APP_{swe}/PS1_{\Delta E9}$ mouse model of AD which has mutations in APP and presenilin-1 (PS1); as well as the human AD retina. They detected retinal Aβ plaques in the mouse model of AD which were co-labelled with curcumin and a variety of anti-Aβ antibodies. Plaques were detected in almost all layers of the retina including NFL, GCL, IPL, INL, OPL, ONL and in the sclera of the transgenic mice eyes. Retinal plaques were detected in mice as young as 2.5 months old and when comparing retinal and cerebral pathology, retinal plaques occurred prior to those within the brain and increased with age and disease progression. As previously mentioned, they also managed to image retinal Aβ plaques in vivo in live transgenic mice using curcumin. Perez et al. (2009) detected retinal Aβ deposits in the same mouse model of AD ($APP_{swe}/PS1_{\Delta E9}$) using anti-Aβ antibodies and thioflavin-S; a dye which stains fibrillar amyloid. Mice were aged 12-19 months and majority of plaques were found in the IPL and OPL of the retina. The plaques increased in number and size as the mice aged. They concluded that retinal plaques were similar in structure to those located within the brain of the same mice suggesting that retinal pathology correlates with brain pathology in AD. Consistent with these findings were results from another study investigating the same transgenic mouse model of AD. Mice of age 13-16 months were subjected to anti-Aβ antibodies and thioflavin-S staining. An increase in Aβ deposition was evident, as well as a number of other degenerative changes in the retina when transgenic mice were compared to wildtype mice. These included a loss of neurones in the GCL, thinning of the IPL and a reduction in the axons of the optic nerve (Gupta et al., 2016). The presence of Aβ deposits was detected in the NFL and GCL of the retina and within retinal and choroidal vasculature in another research study which investigated two different APP/PS1 mouse models of AD using an anti-Aβ antibody. Transgenic mice were aged between 7-27 months and an increase in Aβ load was apparent when comparing mice of age 7 months and 27 months. This study also detected a loss of neuronal cells within the GCL of retinas from transgenic mice which is characteristic of the neurodegeneration present in AD (Ning et al., 2008). Another study investigating transgenic mouse models of AD, found Aβ deposits in 14 month old Tg2576 mice. Aβ deposits were located in the neural retinal layers from GCL to ONL using anti-Aβ antibodies including the 6E10 antibody. Retinal thickness was decreased in transgenic mice, showing loss of cells within the retina (Liu et al., 2009). A possible Aβ labelling was detected in the GCL, INL, lens and cornea in an analysis of two mouse models of AD (Tg2576 and $APP_{swe}/PS1_{\Delta E9}$) using anti-Aβ antibodies (Dutescu et al., 2009). Finally, Tsai et al. (2014) found Aβ plaque-like structures in the retina of eyes from a transgenic rat model of AD. These were located in the IPL, OPL & choroid

using the 6E10 antibody. A number of different pathologies related to AD have been identified in transgenic animal models. Transgenic animals are useful in research to model different aspects of AD; however, it must be acknowledged that they are not completely representative of how this complex and progressive disease would manifest in humans.

Similar AD-associated pathologies have been detected in the retina of both human AD patients and transgenic animal models of AD. These include Aβ deposition, loss of neurones, thinning of retinal layers and degeneration of the optic nerve. If pathogenic changes characteristic of AD can be identified successfully in the retina and they are representative of brain pathology, the retina would provide an ideal target for diagnosis and monitoring of AD. Aβ accumulation has been described as the initiating event in AD pathogenesis (Hardy and Higgins, 1992), therefore much interest has been paid to its identification within the retina. My research has focused mainly on Aβ deposition within the retina of humans and transgenic mouse models of AD. In the interest of the vascular hypothesis for AD onset (De La Torre, 2002; De La Torre, 2004), I visualised the retinal vasculature to investigate if a relationship exists between Aβ and the retinal blood vessels.

Aims & Purpose of the Research

AD is a complex, neurodegenerative condition which results in degeneration of the brain. Its pathogenesis is poorly understood. As a result, numerous clinical challenges have arisen in the diagnosis and monitoring of the condition. Novel methods which can detect AD-associated pathologies in the presymptomatic stage of the disease are urgently needed to aid an earlier diagnosis. It has been proposed that retinal pathology may represent brain pathology given the direct link between the two structures (Lim et al., 2016). The eye has advantages over the brain as it can be easily assessed, imaged non-invasively and inexpensively. Therefore detection of abnormal protein deposits associated with AD such as Aβ within the retina of the eye could be a potential answer to the clinical challenges which result from the condition.

The aims of my research were:

1. To identify Aβ within the retina of AD patients and transgenic mouse models of AD
2. To investigate the relationship between Aβ and the retinal vasculature

To investigate these factors I analysed the retinas from eyes of human AD patients and age-matched controls and from transgenic mouse models of AD and their wildtype littermates by immunohistochemistry techniques in order to identify Aβ deposits and their relation with retinal blood vessels.

Methods

Project Design

My project included research on retinal tissue from human and transgenic mouse models of AD. I aimed to investigate Aβ accumulation within the retina and how it was related to retinal vasculature.

Initially I began my research on human tissue; first optimisation of the vascular labelling was carried out on non-AD samples. I then moved on to explore the detection of retinal Aβ in both non-AD and AD eyes. A number of different conditions were explored in the attempt to identify Aβ accumulations within the retina including antibodies and dyes specific to Aβ, antibody concentrations, incubation times and antigen retrieval methods. Despite detecting Aβ in other areas of the eye, difficulties were experienced in the detection of Aβ within the neural retinal layers.

In regards to transgenic mice; I first learned how to dissect the mice eyes to isolate the retina. Similarly to human tissue, next optimisation of the vascular labelling was carried out on the retina of wildtype mice. I then moved on to the identification of retinal Aβ within transgenic and wildtype mice exploring a number of different conditions as with research on human retinal tissue.

Given the positive results found by other experimental studies (La Morgia et al., 2016; Koronyo-Hamaoui et al., 2011); I replicated their protocols in order to attempt to label Aβ deposits within the retina.

Finally I investigated formic acid as an antigen retrieval method on cross-sections of the eyes from human and transgenic mice. Previous antigen retrieval focussed on heat induced citrate buffer, formic acid retrieval was explored as it has been described to enhance Aβ detection (Cummings et al., 2002; D'Andrea et al., 2003).

Human Samples

Human donor eyes were obtained from Moorfields Eye Hospital, London. Eyes were fixed in 4% PFA and stored at 4°C. Donor eyes may lack the cornea due to corneal transplantation. Paraffin-embedded cross-sections of human eyes were obtained from University College London (UCL) Pathology Department, London. Eyes were fixed in 4% PFA, embedded in paraffin and sectioned. Paraffin-embedded sections

were stored at room temperature (RT). Sagittal sections of thickness 4µm and 10µm were used. Brain slices were obtained from Queen Square Brain Bank for Neurological Disorders, UCL, London. Samples were embedded in Optimal Cutting Temperature (OCT) compound, frozen and sectioned. Frozen samples were stored at -80°C. Brain slices of thickness 10µm were used. AD samples were confirmed with the condition upon post-mortem examination of the brain. AD samples and healthy control eyes were age-matched in experiments.

Sample	Control/ AD	Tissue type	Source	Treatment	Age	Sex	Cause of death
1	Control	Flat-mount retina & Bruch's membrane	Moorfields Eye Depository	Fixed in 4% PFA	80	F	Cardiovas-cular disease
2	Control	Cross-section of eye	UCL Pathology Department	Fixed in 4% PFA and embedded in paraffin	84	M	-
3	Control	Cross-section of eye	UCL Pathology Department	Fixed in 4% PFA and embedded in paraffin	-	-	-
4	Control	Cross-section of eye	UCL Pathology Department	Fixed in 4% PFA and embedded in paraffin	-	-	-
5	Control	Cross-section of eye	UCL Pathology Department	Fixed in 4% PFA and embedded in paraffin	85	M	-
6	Control	Brain slice	Queen Square Brain Bank for Neurological Disorders (UCL)	Embedded in OCT compound and frozen	81	-	-
7	Dementia (subtype unknown)	Cross-section of eye	UCL Pathology Department	Fixed in 4% PFA and embedded in paraffin	91	-	-
8	AD	Flat-mount retina	Moorfields Eye Depository	Fixed in 4% PFA	90	-	Pneumon-ia
9	AD	Brain slice	Queen Square Brain Bank for Neurological Disorders (UCL)	Embedded in OCT compound and frozen	79	-	-

Table 1. **Details on human samples.** AD-Alzheimer's disease, UCL-University College London, PFA-paraformaldehyde, OCT-Optimal Cutting Temperature, F-female, M-male, (-) information not available.

Mice Samples

The eyes from 9-month old double mutated transgenic mice and wildtype littermates were obtained from Lundbeck. Mice were the APP/PS1-21 model of AD which harbour mutations in amyloid precursor protein (APP KM670/671NL (Swedish)) and presenilin-1 (PS1 L166P) genes. Presenilin-1 is a core protein found in the γ-secretase complex which is involved in the production of Aβ peptides. Mutations in these genes are associated with early-onset AD and result in elevated Aβ peptides, particularly Aβ42 leading to increased plaque formation. Eyes were fixed overnight in 4% PFA and transferred to phosphate buffered saline (PBS) containing sodium azide and stored at 4°C. Mice eyes obtained from University College London were the APP/PS1 (TASTPM) model of AD. This model has mutations in APP (APP KM670/671NL (Swedish)) and presenilin-1 (PSEN1 M146V) genes. Mice were aged 14-16 months and eyes were perfused fixed with 4% PFA and stored at 4°C. Paraffin-embedded cross-sections of mice eyes obtained from University College London were the APP/PS1 (TASTPM) model of AD, mutations as previously described. Eyes were fixed in 4% PFA, embedded in paraffin and sectioned. Paraffin-embedded sections were stored at RT. Mice were aged 21-25 months and sections were of thickness 10µm.

Sample	WT/TG	Tissue type	Source	Treatment	Age
1	WT	Flat-mount retina	Lundbeck	Fixed in 4% PFA overnight then transferred to PBS containing sodium azide	9 months
2	WT	Flat-mount retina	Lundbeck	Fixed in 4% PFA overnight then transferred to PBS containing sodium azide	9 months
3	TG APP/PS1-21	Flat-mount retina	Lundbeck	Fixed in 4% PFA overnight then transferred to PBS containing sodium azide	9 months
4	WT	Flat-mount retina	UCL	Perfused fixed with 4% PFA	16 months
5	TG APP/PS1 (TASTPM)	Flat-mount retina	UCL	Perfused fixed with 4% PFA	16 months
6	WT	Flat-mount retina	UCL	Perfused fixed with 4% PFA	16 months
7	TG APP/PS1 (TASTPM)	Flat-mount retina	UCL	Perfused fixed with 4% PFA	14 months
8	WT	Flat-mount retina	Lundbeck	Fixed in 4% PFA overnight then	9 months

				transferred to PBS containing sodium azide	
9	TG APP/PS1-21	Flat-mount retina	Lundbeck	Fixed in 4% PFA overnight then transferred to PBS containing sodium azide	9 months
10	WT	Cross-section of eye	UCL	Fixed in 4% PFA and embedded in paraffin	21 months
11	TG APP/PS1 (TASTPM)	Cross-section of eye	UCL	Fixed in 4% PFA and embedded in paraffin	25 months

Table 2. **Details on mice samples.** WT-wildtype, TG-transgenic, APP-amyloid precursor protein, PS1-presenilin-1, UCL-University College London, PFA-paraformaldehyde, PBS-phosphate buffered saline, (-) information not available.

Dissection & Histological Preparation of Mice & Human Eyes

Both human donor eyes and transgenic mice eyes were initially washed 2 times for 5 minutes with PBS. To generate sections of flat-mount retina, the anterior portion of the eye was removed and retina isolated by dissection. Vitreous humour was removed as much as possible manually unless stated otherwise. Where enzymatic treatment was used to digest vitreous humour, tissue was treated with hyaluronidase (type I-S) for 10-30 minutes then washed three times for 10 minutes with phosphate buffered saline (PBS) (Koronyo-Hamaoui et al. 2011).

Immunohistochemistry in Mice and Human Tissue

Deparaffinization

Tissues are embedded in paraffin wax to preserve tissue morphology, this wax must be removed before immunohistochemistry. Paraffin-embedded cross-sections of eyes were deparaffinised through a series of xylenes, hydrated through 100%, 90% and 70% ethanol solutions and washed in distilled water. Next cross-sections were washed with washing buffer (PBT - PBS containing 0.1% Triton X-100, 0.5% bovine serum albumin (BSA), 1mM $CaCl_2$ and 1mM $MgCl_2$). Washing buffer was used in all washes unless otherwise stated. $CaCl_2$ and $MgCl_2$ was present in all samples which vasculature was labelled.

Antigen Retrieval & Blocking

The fixation process is necessary to preserve the tissue structure however cross-links form between proteins during this process and this masks antigenic sites within the

tissue. Antigen retrieval can be used to expose epitopes, allowing antibodies to bind. Where antigen retrieval was used, flat-mount retinal samples were subjected to 9 minutes at 96°C in a water bath and cross-sections of eyes and brain slices for 9 minutes in a microwave (900 Watt) avoiding boiling. All experiments with antigen retrieval involved heated citrate buffer apart from one experiment on human and mice cross-sections which investigated formic acid as an antigen retrieval method. A homemade citrate buffer was used (10mM Citric Acid, 0.05% Tween 20, adjusted to pH6.0 using 1M NaOH) unless otherwise stated. As previously mentioned, one experiment was conducted using 70% formic acid. Cross-sections of human and mice eyes were incubated for 10 minutes at RT under a fume hood in this case. Samples were then washed 2 times for 5 minutes with PBT. Samples were blocked with a solution of 5% goat serum diluted in washing buffer to prevent non-specific binding of antibodies and increase the signal-noise ratio. Incubation with blocking solution was for 2 hours at 30°C for flat-mount tissue or 1 hour at RT for cross-sections. Samples were then washed 2 times for 6 minutes in PBT.

In the replicated protocols; the protocol by La Morgia et al. (2016) involved antigen retrieval with modified citrate buffer (pH 6.0) diluted (1:10) in distilled water for 1 hour at 96°C. Human samples were blocked with PBS containing 20% goat serum and 0.05%Triton X-100 for 1 hour at RT. The protocol by Koronyo-Hamaoui et al. (2011) involved antigen retrieval with modified citrate buffer (pH 6.0) diluted (1:10) in distilled water for 9 minutes at 96°C. Human and mice samples were blocked with PBS containing 20% goat serum and 0.05% TritonX-100 for 1 hour at RT.

Immunolabelling in Human Tissue

During various experiments flat-mount retinal or Bruch's membrane samples may have been incubated with a combination of primary antibodies including anti-Aβ mouse monoclonal antibody 6E10 (1:100), anti-Aβ rabbit polyclonal antibody CN3 (1:1000) and biotinylated Ulex europaeus agglutinin-I (UEA-I) (1:100) diluted in PBT. Incubations were for 4 hours at 30°C or overnight at 4°C. Temperature was increased in order to make the tissue more permeable or a longer incubation time was to allow more time for penetration of the antibody into the tissue. Samples were then washed 8 times for 5 minutes. Efficient washing removes any unbound antibodies to prevent non-specific signal. Secondary antibodies included Alexa Fluor 488 goat anti-mouse IgG1 (1:200), Alexa Fluor 546 goat anti-rabbit IgG (H+L) (1:200) and Alexa Fluor 647 streptavidin conjugate (1:200) diluted in PBT. Incubation time with secondary antibodies was for 2 hours at 30°C. Samples must be kept in dark conditions from

addition of the secondary antibody. Samples were then washed 8 times for 5 minutes with PBT.

Cross-sections of human eyes may have been incubated with anti-Aβ mouse monoclonal antibody 6E10 (1:100), and biotinylated UEA-I (1:100) for 1 hour at RT or 2 hours at 30°C. Samples washed 3 times for 5 minutes with PBT. Secondary antibodies included Alexa Fluor 488 goat anti-mouse IgG1 (1:200) and Alexa Fluor 647 streptavidin conjugate (1:200). Incubations were for 1 hour at RT or 2 hours at 30°C. Samples washed 3 times for 5 minutes with PBT.

Brain slices were incubated with anti-Aβ antibody 6E10 diluted in PBT for 1 hour at RT. Washed 3 times for 5 minutes. Secondary antibody used was Alexa Fluor 488 goat anti-mouse IgG1 (1:200) diluted in PBT and incubated for 1 hour at RT. Washed 3 times for 5 minutes. Then stained with curcumin solution (2 mg curcumin in 2 drops of NaOH) diluted in PBS to make a concentration 0.1 mg/ml. Incubated for 10 minutes at RT then washed 3 times for 5 minutes in PBS.

In replicated protocols; the protocol by La Morgia et al. (2016) involved primary antibodies which were diluted in PBS with 2% blocking solution and incubated for 72 hours at 4°C. Secondary antibodies were diluted in PBS and incubated for 1 hour at 37°C. All washes were as previously mentioned but with PBS. The protocol by Koronyo-Hamaoui et al. (2011) involved primary antibodies which were diluted in PBS containing 10% blocking solution for 48 hours at 4°C. Secondary antibodies were diluted in PBS and incubated for 1.5 hours at RT. Samples were then treated with 0.3% Sudan Black B (SBB) diluted in 70% ethanol for 10 minutes at RT. Samples were washed 3 times for 5 minutes in 70% ethanol and 2 times for 5 minutes in PBS. Next samples were labelled with curcumin solution (2 mg curcumin in 2 drops of NaOH) diluted in PBS to make a concentration 0.1 mg/ml. Incubated for 10 minutes at RT then washed 3 times for 15 minutes in PBS. All other washes were as previously mentioned but with PBS.

Nuclei was stained with 4',6-diamidino-2-phenylindole dihydrochloride (DAPI) (1:1000) for 15 minutes at RT for cross-sections and brain slices and 30 minutes at RT for flat-mount tissue. One experiment involved HAP labelling using Osteosense (1:10) which was added with DAPI. Samples were washed for 3 times for 5 minutes for cross-sections or 5 times for 5 minutes for flat-mount tissue in PBS and mounted using Vectashield containing No DAPI. Coverslips were added and sealed with nail varnish. Slides were stored in dark conditions at 4°C after immunostaining procedure.

Immunolabelling in Mouse Tissue

Flat-mount retinal samples from mice may have been incubated with a combination of primary antibodies including anti-Aβ mouse monoclonal antibody 6E10 (1:100), anti-tau rabbit polyclonal antibody (1:1000) and biotinylated Isolectin-B4 (1:100) for 4 hours at 30°C. Washed 8 times for 5 minutes with PBT. Secondary antibodies included Alexa Fluor 488 goat anti-mouse IgG1 (1:200), Alexa Fluor 568 streptavidin conjugate (1:200), Alexa Fluor 647 streptavidin conjugate (1:200) and Alexa Fluor 546 goat anti-rabbit IgG (H+L) (1:200). Incubation time for secondary antibodies was for 2 hours at 30°C. Samples washed 8 times for 5 minutes with PBT. DAPI staining and mounting as previously mentioned.

Cross-sections of mice eyes were incubated with anti-Aβ mouse monoclonal antibody 6E10 (1:100) and biotinylated Isolectin-B4 (1:100) for 1 hour at RT. Samples washed 3 times for 5 minutes with PBT. Secondary antibodies included Alexa Fluor 488 goat anti-mouse IgG1 (1:200) and Alexa Fluor 647 streptavidin conjugate (1:200). Incubation was for 1 hour at RT. Samples were then washed 3 times for 5 minutes with PBT. DAPI staining and mounting as previously mentioned.

In replicated protocol by Koronyo-Hamaoui et al. (2011); primary antibodies which were diluted in PBS containing 10% blocking solution and incubated overnight at 4°C. Secondary antibodies were diluted in PBS and incubated for 1 hour at RT. Samples washed as previously mentioned in PBS. DAPI staining and mounting as previously mentioned.

In all experiments negative controls were treated with an identical protocol however with omission of primary antibody to assess non-specific binding. Where the association with Aβ deposits and retinal vasculature was investigated, vasculature markers were used in negative controls.

Reagent	Source
1X Phosphate Buffered Saline (PBS) (pH7.4)	Gibco (10010-015)
Triton X-100	Sigma-Aldrich (MKBW8386)
Bovine Serum Albumin (BSA)	Sigma-Aldrich (A7906)
Hyaluronidase (type-1)	Sigma-Aldrich (H3506)
Citric acid, anhydrous	Sigma-Aldrich (251275)
Tween-20	Sigma-Aldrich (P1379)
Sodium hydroxide (NaOH)	Sigma-Aldrich (221465)
Citrate Buffer (modified)	DAKO (S1699)
Formic Acid	Fisher Scientific (F/1900/PB15)
Goat serum	Sigma-Aldrich (G9023)
$CaCl_2$	Sigma-Aldrich (C-4901)
$MgCl_2$	BHD (101494V)
Vectashield (NO DAPI)	Vector Labs (H-100)

Table 3. **List of reagents used in immunohistochemistry.**

Immunolabelling agents	Type	Dilution	Source
6E10 for Aβ (amino acid residue 1-16)	Mouse monoclonal antibody	(1:100)	Covance (Sig-39320)
CN3 for Aβ (amino acid residue 1-16)	Rabbit polyclonal antibody	(1:1000)	Tubingen
Curcumin for Aβ	Dye	(1:20)	Sigma-Aldrich (C1386)
Ulex Europaeus Agglutinin-I (UEA-I) for human vasculature (fucose and arabinose)	Biotin conjugated lectin	(1:100)	Vector Labs (B-1065)
Isolectin B4 for murine vasculature (α-D-galactosyl residues)	Biotin conjugated lectin	(1:100)	Vector Labs (L2140)
Anti-human Tau	Rabbit polyclonal antibody	(1:1000)	DAKO (A0024)
Alexa Fluor 488 goat anti-mouse IgG1	Goat polyclonal antibody	(1:200)	Invitrogen (A-21121)
Alexa Fluor 546 goat anti-rabbit IgG (H+L)	Goat polyclonal antibody	(1:200)	Invitrogen (A-11010)
Streptavidin, Alexa Fluor 647 conjugate	Streptavidin	(1:200)	Invitrogen (S21374)
Streptavidin, Alexa Fluor 568 conjugate	Streptavidin	(1:200)	Invitrogen (S11226)

OsteoSense 680EX for hydroxyapatite (HAP)	Dye	(1:10)	Perkin Elmer (NEV10020EX)
Sudan Black B	Dye	0.03%	Sigma-Aldrich (199664)
DAPI	Dye	(1:1000)	Thermo Scientific (62248)

Table 4. **List of immunolabelling agents used in immunohistochemistry.**

Microscopy

Results were obtained using Leica Sp8 confocal microscope and LAS AF Leica Confocal Imaging Software. Optimal settings were established for each individual channel used. When optimal microscope settings were established, these settings were used to take all images during individual experiments. When no specific signal was being detected in the red channel, it may have been utilised to view tissue architecture and autofluorescence. During viewing on the microscope, the whole tissue was analysed and representative images were taken. In regards to the analysis of flat-mount tissue, when assessing different conditions in an experiment the same region of the retina was imaged in each case. Fluorescent images were taken with 20X dry, 40X oil, 63X oil and 100X oil objective lens. Associations of specific labelling were distinguished by visual analysis and analysed in depth for specificity. The different channels used were merged to form a final image. Scale bars were applied on fluorescent images and processing was done using Adobe Photoshop CS6. For consistency, any vascular labelling detected with Alexa Fluor 568 streptavidin conjugate was changed to magenta colour in representative images.

Results

Human - Cross-sections of Eyes

In order to investigate how Aβ was related to the retinal vasculature, the retinal blood vessels needed to be visualised. To determine the best concentration for retinal vascular labelling in human tissue, a series of different concentrations of a human vascular marker were investigated. Figure 5 shows results from cross-sections of an eye from a healthy control individual labelled using Ulex europaeus agglutinin–I (UEA-I) (magenta) concentrations (1:50), (1:500) and (1:1000). One cross-section from the same eye was used as a negative control and was treated with PBT instead of UEA-I to assess non-specific binding. When a cross-section of the human eye was labelled with (1:50), retinal and choroidal vasculature is clearly labelled (Fig.5A & E). Retinal layers can be distinguished by the nuclear labelling with DAPI (blue), blood vessels are labelled within the ganglion cell layer (GCL) and inner nuclear layer (INL) (Fig.5A). Vascular labelling was detected in the choriocapillaris (CC) and larger vessels within the choroid (Fig.5E). The cross-section labelled with UEA-I concentration of (1:500) portrays faint labelling of blood vessels in the retina and choroid (Fig.5B & F) and relatively no vasculature labelling can be seen with a UEA-I concentration of (1:1000) (Fig.5C & G). No retinal or choroidal vasculature labelling can be seen in negative controls of retina and choroid (Fig.5D & H). Based on these findings, an efficient UEA-I concentration for vasculature labelling was determined to be between (1:50) and (1:500). As a result, all further human vasculature was visualised using a UEA-I concentration of (1:100).

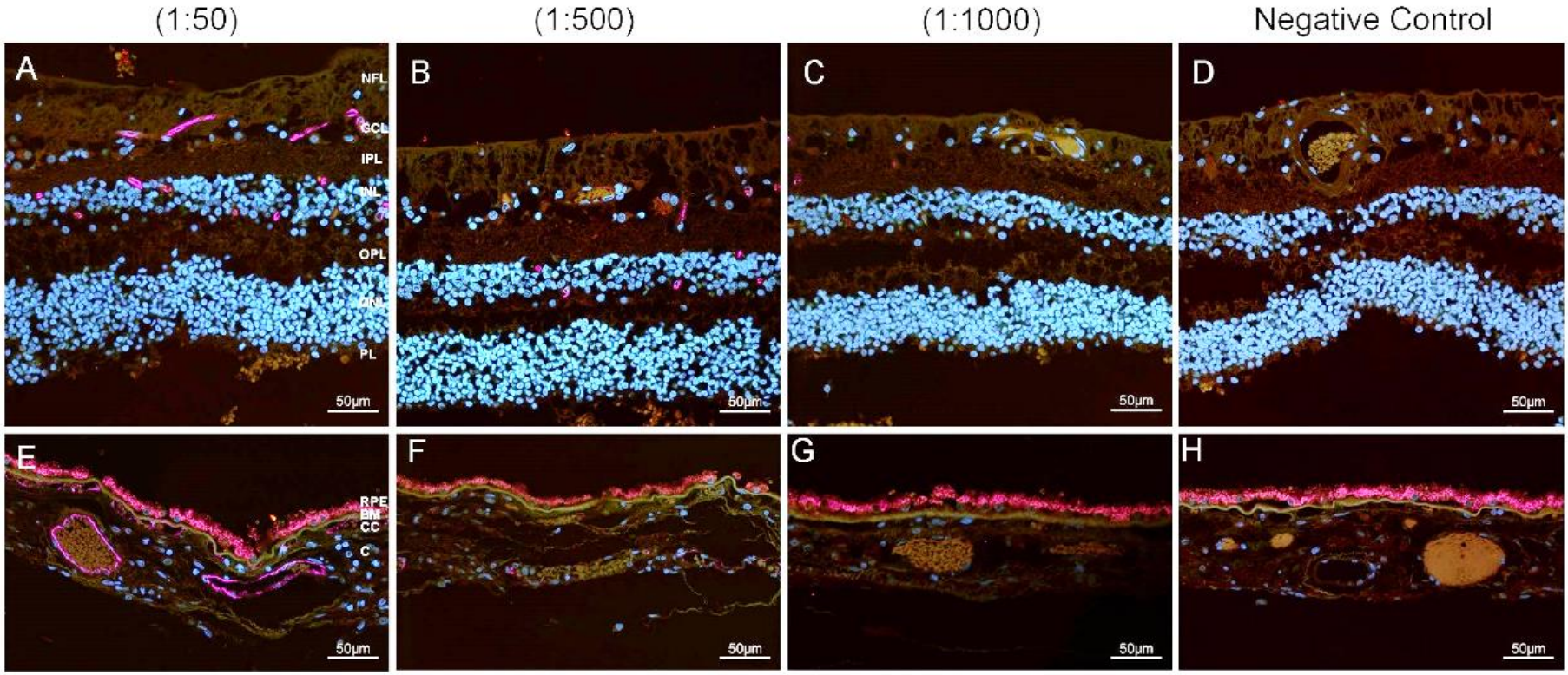

Figure 5. **UEA-I lectin optimisation experiment on cross-sections from a healthy control human eye.** Sections stained with vascular marker: UEA-I (magenta) and nuclei marker: DAPI (blue). (A-D) Representative images of retina and (E-H) of choroid at various UEA-I concentrations. (A & E) UEA-I concentration of (1:50), (B & F) UEA-I concentration of (1:500), (C & G) UEA-I concentration of (1:1000) and (D & H) negative controls images of retina and choroid respectively. NFL-nerve fiber layer, GCL-ganglion cell layer, IPL-inner plexiform layer, INL-inner nuclear layer, OPL-outer plexiform layer, ONL-outer nuclear layer, PL-photoreceptor layer, RPE- retinal pigment epithelium, BM-Bruch's membrane, CC-choriocapillaris and C-choroid.

Next cross-sections of an eye from a healthy control individual were immunolabelled with an anti-Aβ antibody to detect Aβ. Spherical structures (spherules) within drusen were labelled with the anti-Aβ antibody (Figure 6). These cross-sections were subjected to 9 minutes of antigen retrieval with heated citrate buffer and labelled with the anti-Aβ monoclonal antibody 6E10, human vasculature marker UEA-I and nuclei stain DAPI. Aβ labelling was detected within drusen (arrow) and a vast amount of labelling was detected within the sclera (S) (Fig.6A). The same druse at a higher magnification shows numerous spherical forms of Aβ labelling (Fig.6B). No Aβ aggregates were detected in the retinal layers with the 6E10 antibody (Fig.6D). To assess the specificity of the secondary antibody for the 6E10 antibody, the negative control cross-section was subjected to vasculature labelling with UEA-I but no 6E10 was used. No Aβ labelling was detected within the negative control cross-section (Fig.6C & E). Blood vessels (magenta) can be seen throughout the choroid and retina and autofluorescence of RPE is present due to lipofuscin molecules.

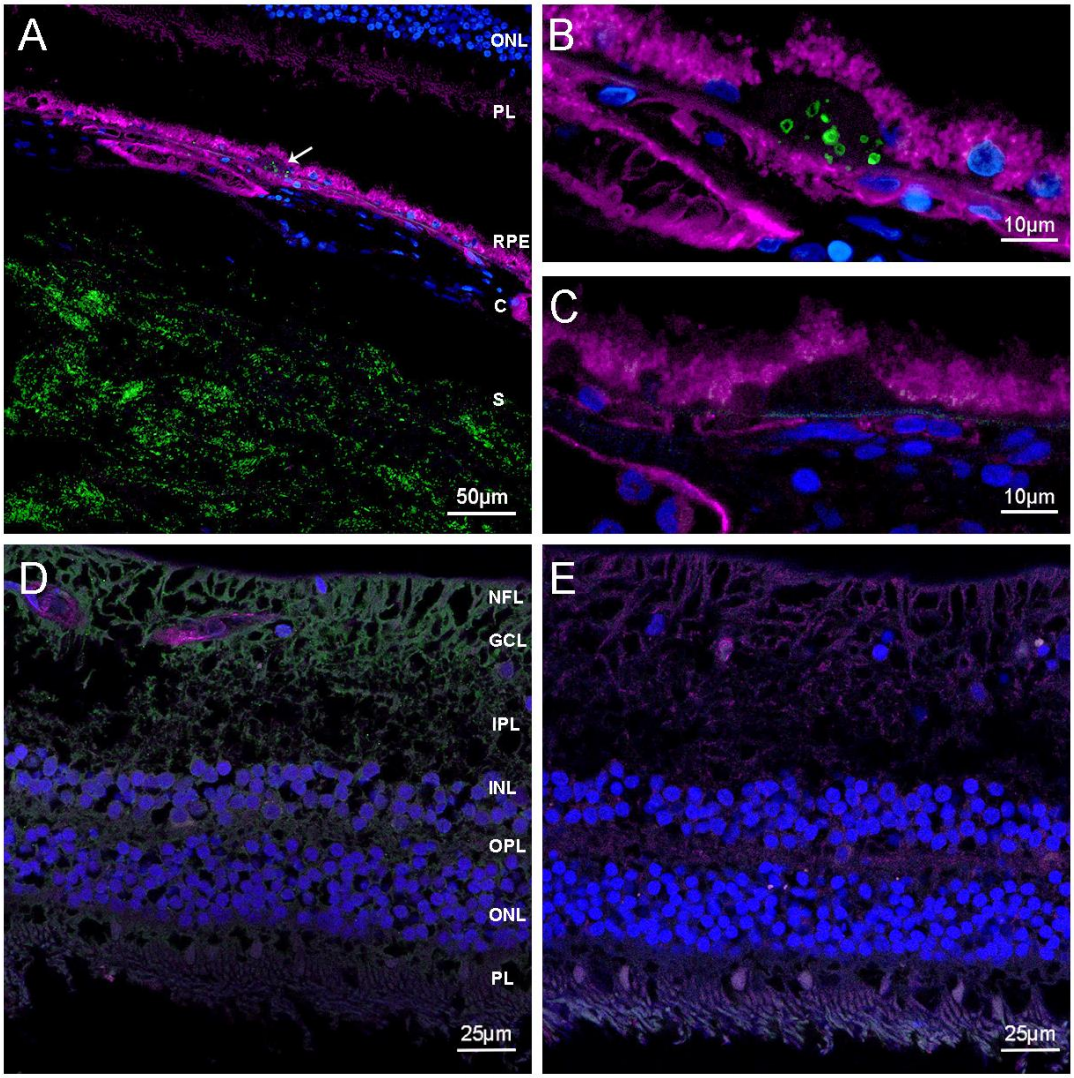

Figure 6. **Amyloid beta (Aβ) staining on cross-sections of a healthy control human eye.** Cross-sections were stained with anti-Aβ antibody: 6E10 (green), vasculature marker: UEA-I (magenta) and nuclei marker: DAPI (blue). (A) Representative image of Aβ labelling detected within druse (arrow) and sclera. (B) Higher magnification image of spherical Aβ labelling within druse. (C) No labelling was detected in drusen in the negative control cross-section. (D) No Aβ plaque-like accumulations were detected in the retina. (E) Negative control image of the retina. NFL-nerve fiber layer, GCL-ganglion cell layer, IPL-inner plexiform layer, INL-inner nuclear layer, OPL-outer plexiform layer, ONL-outer nuclear layer, PL-photoreceptor layer, RPE-retinal pigment epithelium, C-choroid and S-sclera.

Antigen retrieval is used to unmask epitopes and allow antibodies to bind more efficiently to proteins of interest. Different antigen retrieval incubation times with heated citrate buffer were investigated shown in Figure 7. Cross-sections from a human control eye were subjected to 3, 6, 9 and 18 minutes of antigen retrieval with heated citrate buffer. A negative control slide was subjected to 9 minutes of antigen retrieval and processed exactly as the other slides with omission of the anti-Aβ antibody 6E10. A progressive increase in 6E10 labelling was detected in the retina, drusen and sclera of cross-sections as antigen retrieval time was increased. Cross-sections which were subjected to 3 and 6 minutes of antigen retrieval show slight background labelling of 6E10 antibody in the retina (Fig.7A and D), 9 minutes antigen retrieval increases labelling of the whole tissue (Fig.7G) and 18 minutes shows a dense labelling of the whole tissue (Fig.7J). No Aβ labelling within the retinal layers was deemed specific from these images. No 6E10 labelling was detected in the negative control retina (Fig.7M). Within drusen, spherules were labelled in cross-sections subjected with 3-18 minutes of antigen retrieval (Fig.7B, E, H and K). In regards to the sclera, an increase in 6E10 labelling was detected as antigen retrieval time increased (Fig.7 C, F, I and L). When comparing 6E10 labelling in drusen and sclera to retinal labelling, the labelling within drusen and sclera was deemed specific. This was due to the signal from the 6E10 antibody within drusen and sclera with 3 (Fig.7B and C) and 6 minutes (Fig.7E and F) of antigen retrieval is much stronger than the background signal in retina (Fig.7A and D). No labelling was detected in the retina, drusen or sclera of the negative control cross-section (Fig.3M-O). Vasculature was not analysed in this experiment.

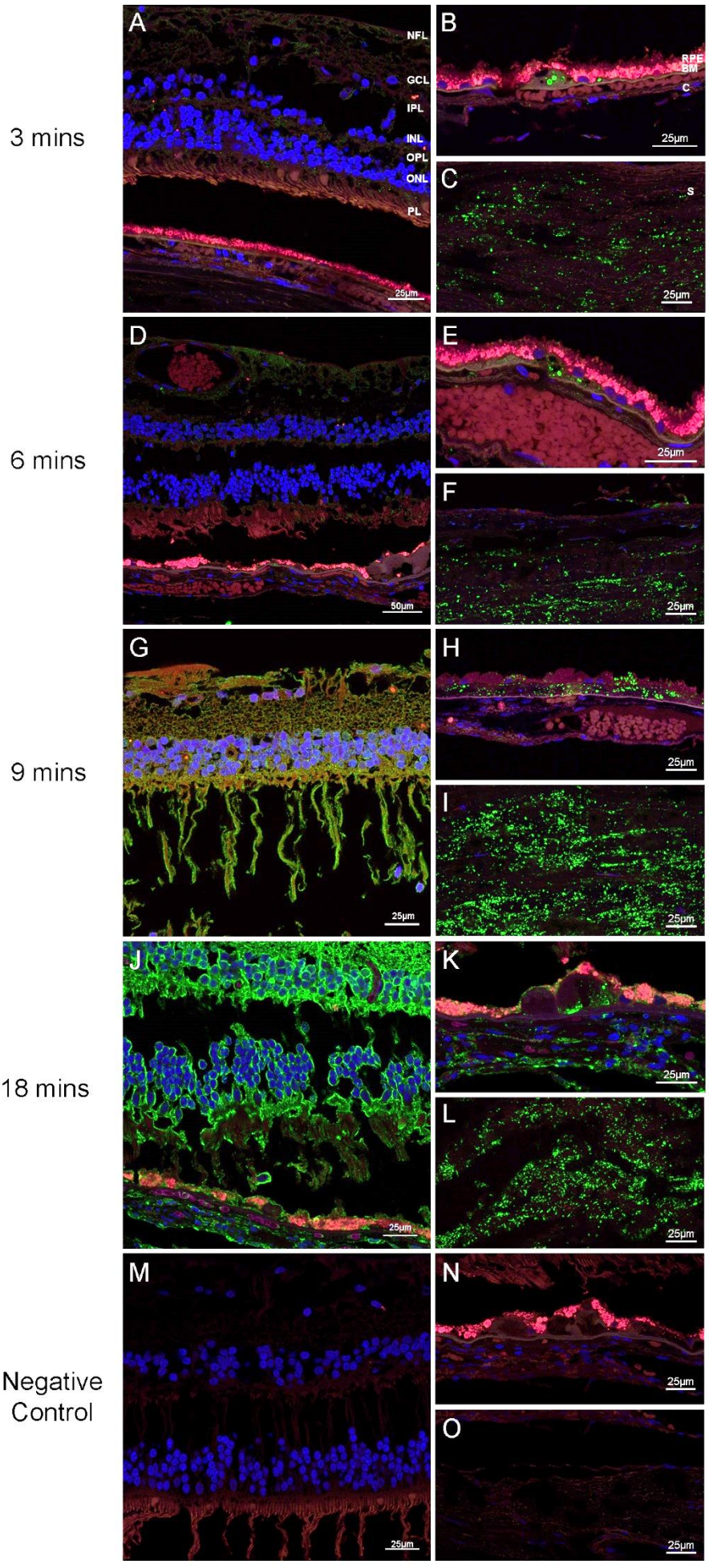
3 mins
6 mins
9 mins
18 mins
Negative Control
A
NFL
GCL
IPL
INL
OPL
ONL
PL
25µm
B
RPE
BM
C
25µm
C
S
25µm
D
50µm
E
25µm
F
25µm
G
25µm
H
25µm
I
25µm
J
25µm
K
25µm
L
25µm
M
25µm
N
25µm
O
25µm

Figure 7. **Different antigen retrieval incubation times with heated citrate buffer on cross-sections from a healthy control human eye.** Cross-sections were stained with anti-Aβ antibody 6E10 and DAPI for nuclei. (A-C) Representative images of 3 minutes incubation time on retina, drusen and sclera respectively, (D-F) 6 minutes incubation time, (G-I) 9 minutes incubation time and (J-L) 18 minutes incubation time. An increase in labelling was detected as antigen retrieval incubation time increased. (M-O) Negative control images. No vascular marker was used in this experiment. NFL-nerve fiber layer, GCL-ganglion cell layer, IPL-inner plexiform layer, INL-inner nuclear layer, OPL-outer plexiform layer, ONL-outer nuclear layer, PL-photoreceptor layer, RPE-retinal pigment epithelium, BM-Bruch's membrane, C-choroid and S-sclera.

Cross-sectional samples from a healthy control eye were stained with the anti-Aβ antibody 6E10 (green) and Osteosense (magenta), a dye which labels hydroxyapatite (HAP) (Figure 8). HAP was investigated due to its presence in drusen and to explore its association with Aβ (Thompson et al., 2015). Spherical labelling of both Aβ and HAP was present within the choroid (Fig.8A, B and C). The three-dimensional organisation of the spherules labelled for Aβ and HAP can be seen in (Fig.8C). The sclera was labelled with Aβ and HAP (Fig.8D-E). The sclera was more densely labelled with HAP (Fig.8D'') than Aβ (Fig.8D'). In all images HAP labelling appears to be more abundant than Aβ. Co-localisation of HAP & Aβ was detected on individual spherules (arrows) (Fig.8B, C and E). These samples were not subjected to any antigen retrieval methods. Vasculature was not analysed in this experiment.

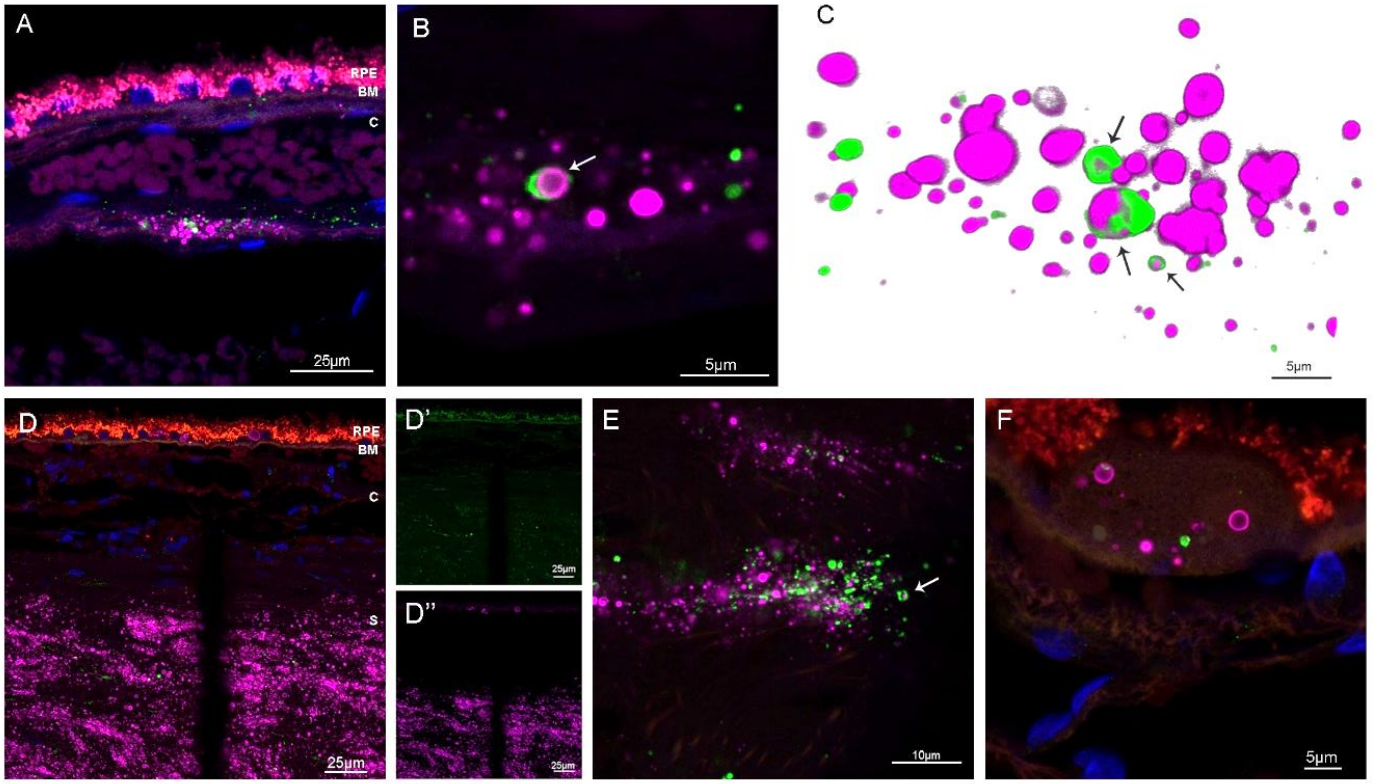

Figure 8. **Aβ and hydroxyapatite (HAP) staining in sub-RPE region of cross-sections from a healthy control human eye.** Sections were labelled with anti-Aβ antibody: 6E10 (green), HAP marker: Osteosense (magenta) and DAPI for nuclei (blue). (A) Representative image of Aβ and HAP labelling detected in choroid. (B) Higher magnification of Aβ and HAP labelling in the choroid. (C) Three-dimensional image of spherical structures labelled with Aβ and HAP. (D & E) Sclera labelling. (D') and (D'') images of separate channels of Aβ and HAP labelling respectively. (F) Aβ and HAP labelling detected within drusen. Co-labelling of Aβ and HAP detected on single spherules (arrows). RPE-retinal pigment epithelium, BM-Bruch's membrane, C-choroid and S-sclera.

An intracellular Aβ labelling was detected in the GCL of the retina (Figure 9). Cross-sections from a healthy control human eye were subjected to the series of different antigen retrieval incubation times with heated citrate buffer as in Figure 7. The intracellular anti-Aβ antibody 6E10 (green) labelling was detected in ganglion cells at 9 and 18 minutes (Fig.9A and B) of antigen retrieval. This labelling was detected in the optic disc area to mid peripheral retina. Nerve fibers also appeared to be labelled at an area near the optic nerve (Fig.9C). This intracellular labelling appears to be distinct from melanopsin ganglion cell (arrow) autofluorescence which appear with red pigments (Fig.9E). No intracellular ganglion cell labelling was detected in the retina when subjected to 3 (Fig.9F) or 6 minutes (Fig.9G) of antigen retrieval or in the negative control (Fig.9H). No Aβ plaque-like accumulations were detected within the retinal layers.

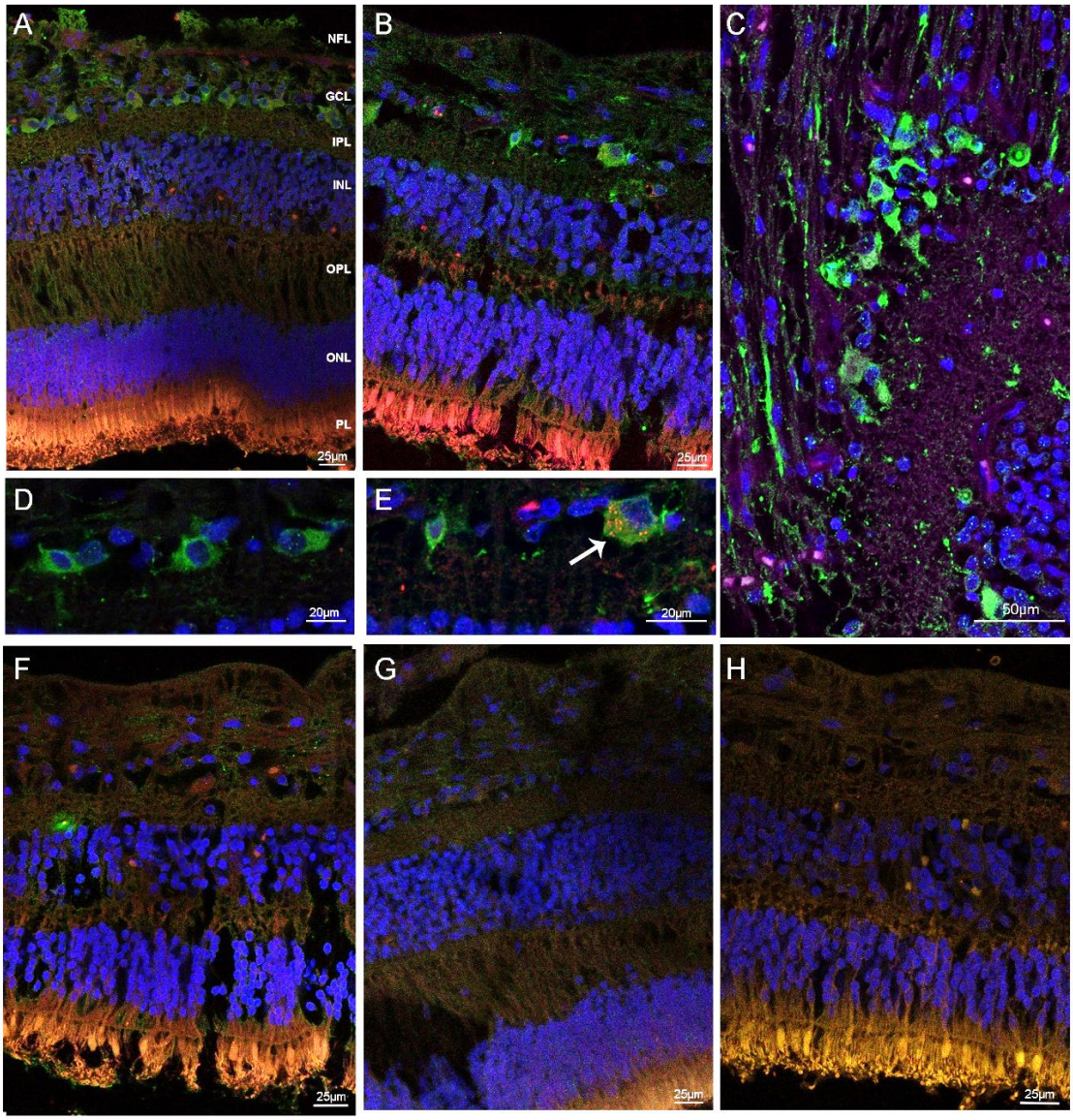

Figure 9. **Ganglion cell labelling in cross-sections of a healthy control human eye.** Cross-sections were subjected to different antigen retrieval incubation times as in Figure 7. Sections were stained with anti-Aβ antibody 6E10 (green) and DAPI for nuclei staining (blue). Aβ labelling was detected in cell bodies of cells located within the ganglion cell layer (GCL) of the retina in cross-sections which were treated to 9 and 18 minutes of antigen retrieval with heated citrate buffer (A & B respectively). (C) Aβ labelling also detected in cell bodies and nerve fibers at an area near the optic disc. (D & E) Higher magnification images of cell body labelling, intracellular Aβ labelling is distinct from melanopsin ganglion cells which present red pigments (arrow). No labelling within the GCL was detected in cross-sections which were subjected to 3 (F) and 6 (G) minutes of antigen retrieval or in the negative control (H). NFL-nerve fiber layer, GCL-ganglion cell layer, IPL-inner plexiform layer, INL-inner nuclear layer, OPL-outer plexiform layer, ONL-outer nuclear layer and PL-photoreceptor layer.

Next replication of a protocol from a publication which reported success in the identification of Aβ plaques within the retina of both AD and healthy control eyes was carried out. I compared three different protocols on cross-sections from a healthy control human eye. All samples were subjected to antigen retrieval with either homemade or a modified citrate buffer depending on the protocol used. The first protocol used was one in which I previously obtained Aβ labelling within drusen (Fig.6). Similarly to previous findings, spherical structures were present in drusen (Fig.9D) with the 6E10 antibody but no labelling was detected in retinal layers (Fig.9A). The next protocol was one in which I previously got labelling within the retinal vessels in flat-mount retina (Fig.12). Results were similar to the previous protocol with Aβ labelling detected within drusen (Fig.9E) but not within the retina (Fig.9B). The last protocol was a replication from a publication (‘Melanopsin Retinal Ganglion Cell Loss in Alzheimer Disease’ by La Morgia et al. (2016)) which had reported successful identification of Aβ deposits within the retina of AD and age-matched control individuals. This protocol involved a long and harsh antigen retrieval method, which appeared to make the antibodies adhere to the tissue non-specifically. As a result, the whole tissue was labelled and no specific labelling could be detected within the retina and drusen (Fig.9C and F).

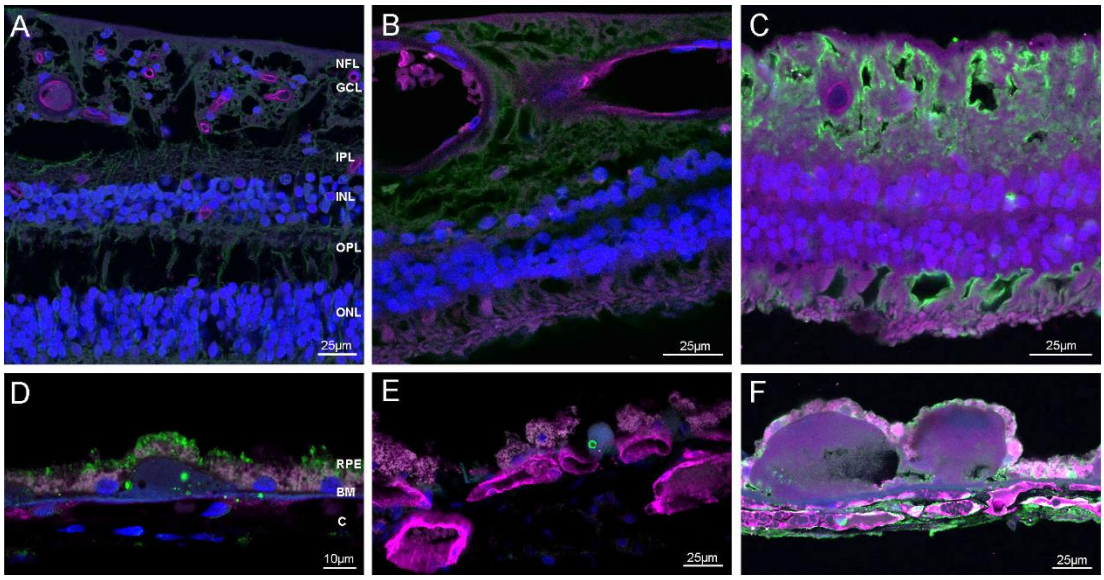

Figure 10. **Comparison of three different protocols of Aβ immunostaining on cross-sections from a healthy control human eye.** Sections were stained with anti-Aβ antibody: 6E10 (green), vasculature marker: UEA-I (magenta) and DAPI for nuclei staining (blue). (A-C) Representative images of retina and (D-F) drusen. (A & D) Protocol 1 – where previous Aβ labelling was detected in drusen (Fig.6). No Aβ labelling was detected in the retina (A), Aβ labelling was detected within drusen (D). (B & E) Protocol 2 – where Aβ labelling was detected within flat-mount retinal tissue (Fig.12). No Aβ labelling detected in the retina (B), Aβ labelling was detected within drusen (E). (C & F) Protocol 3 – adapted from a publication ('Melanopsin Retinal Ganglion Cell Loss in Alzheimer Disease' by La Morgia et al. (2016)). Whole tissue appears to be labelled within the retina (C) and druse (F). No specific labelling could be detected. NFL-nerve fiber layer, GCL-ganglion cell layer, IPL-inner plexiform layer, INL-inner nuclear layer, OPL-outer plexiform layer, ONL-outer nuclear layer, RPE-retinal pigment epithelium, BM-Bruch's membrane and C-choroid.

All previous antigen retrieval methods have focused around the heated citrate buffer method. Towards the end of my project I investigated another method of antigen retrieval; formic acid. Figure 11 shows results from cross-sections of the eyes from an individual who suffered from dementia (subtype was unknown) and an age-matched control individual. Samples were treated with heated citrate buffer (Fig.11A-F), formic acid (Fig.11G-O) or no antigen retrieval (Fig.11P-S). Citrate buffer was used as a positive control as we know from previous results that Aβ labelling is present in drusen and sclera with heat induced antigen retrieval using citrate buffer. Similar to previous results, Aβ was detected in drusen both within the dementia sample (Fig.11B and C) and age-matched control (Fig.11F). Spherules labelled with Aβ are also present beneath Bruch's membrane (Fig.11F). Intracellular Aβ labelling was detected within the retina of the age-matched control sample (Fig.11D and E) but not in the retina of the dementia sample (Fig.11A). Similarly to the previous ganglion cell labelling, this labelling was only apparent near the optic disc area to mid periphery of

the retina. In the samples which were treated with formic acid, Aβ labelling was detected in an area of the retina in the age-matched control sample (Fig.11K and M). This may be an intracellular labelling as previously found or possibly clusters of vascular-related deposits as a vessel is located adjacent to the labelling. To distinguish between a melanopsin ganglion cell and this possible intracellular ganglion cell or vascular-related Aβ labelling, a melanopsin ganglion cell is shown (Fig.11N). Melanopsin ganglion cells autofluoresce with red pigments and the 6E10 labelling is distinct from this autofluorescence which melanopsin ganglion cells present. Formic acid treatment appeared to increase the amount of Aβ labelling within drusen and sclera; however, no Aβ labelling other than that mentioned previously (Fig.11D, E and M) was identified in the retinal layers in the age-matched control or dementia samples. Aβ was detected in drusen in both dementia and age-matched control samples that were not subjected to antigen retrieval (Fig.11Q and S); however, at a lesser quantity than in other antigen retrieved samples. No Aβ was detected in the retinal layers in non-antigen retrieved samples (Fig.11.P and R).

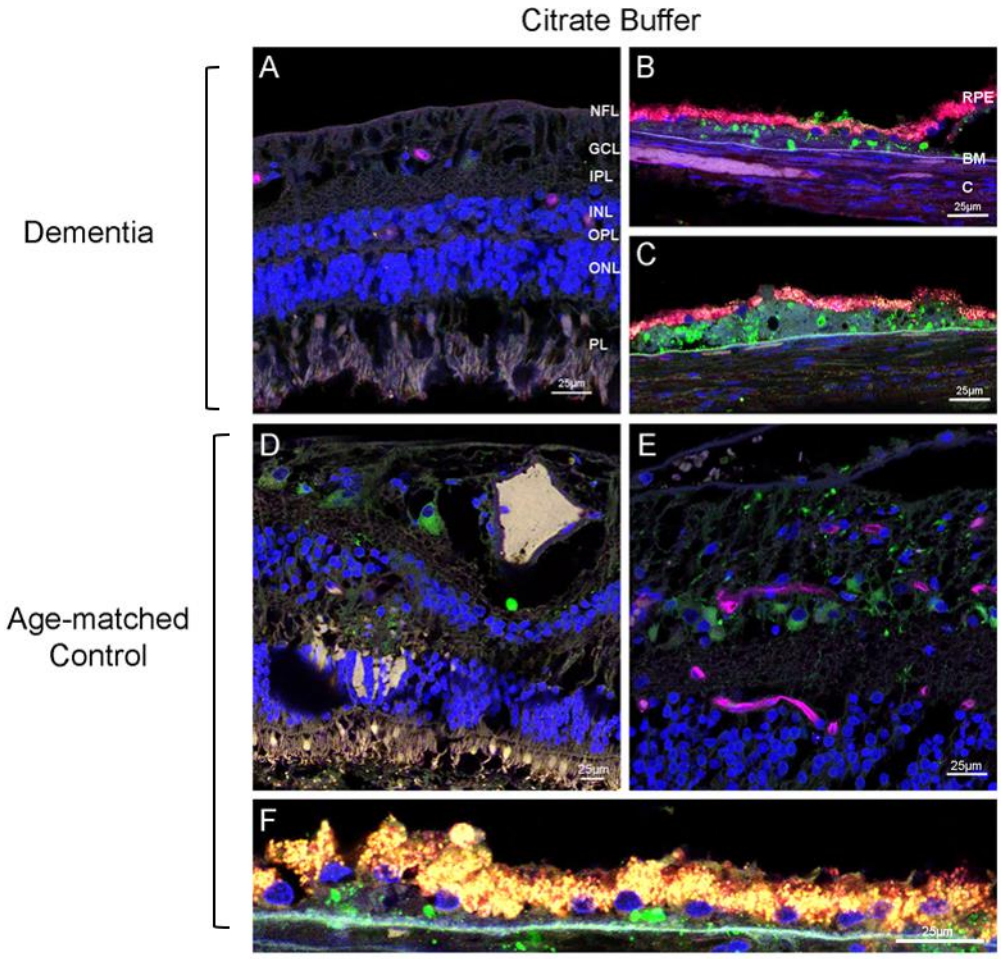

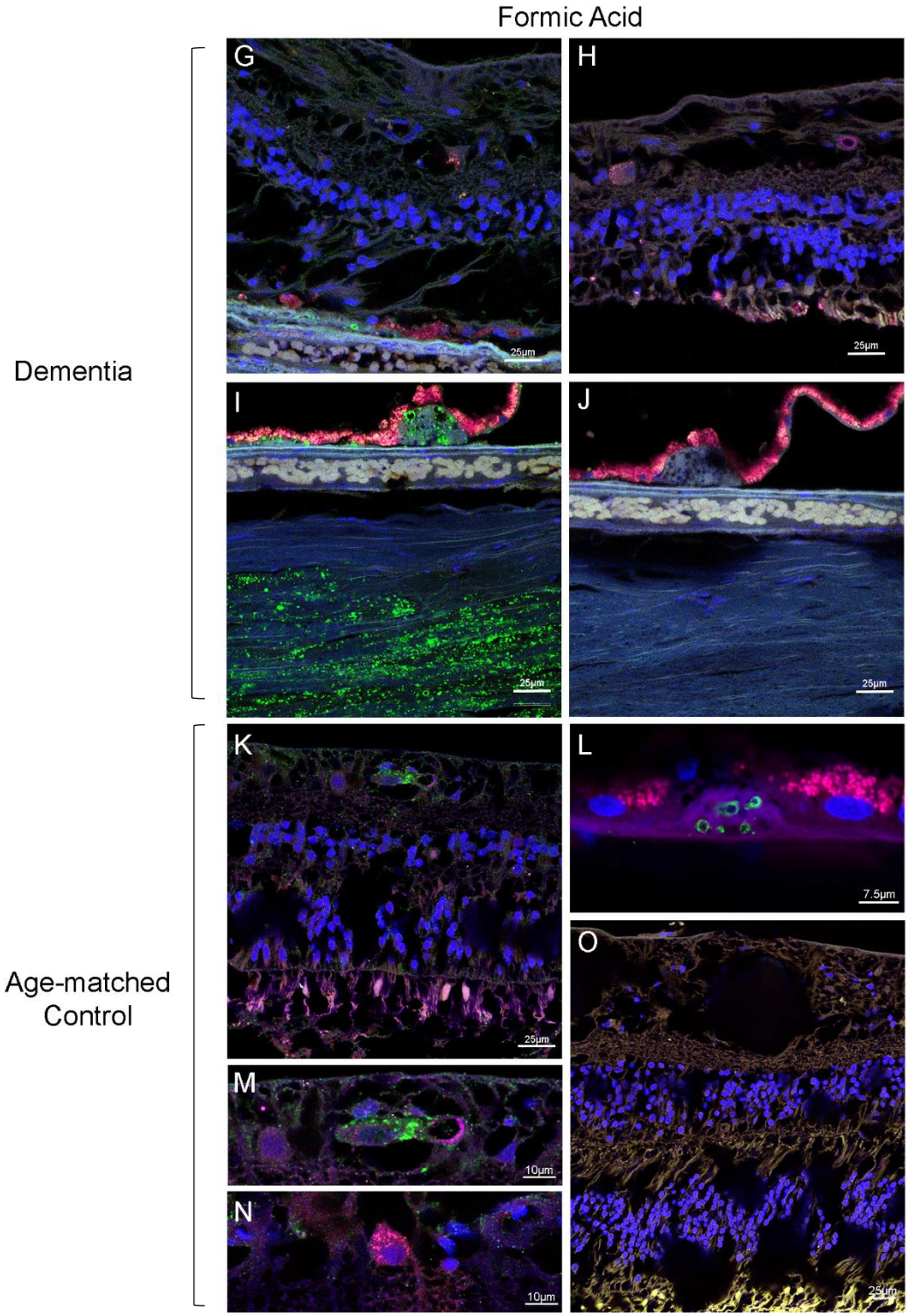
Formic Acid
Dementia
Age-matched Control
G
H
I
J
K
L
M
N
O
25µm
25µm
25µm
25µm
25µm
7.5µm
10µm
10µm
25µm

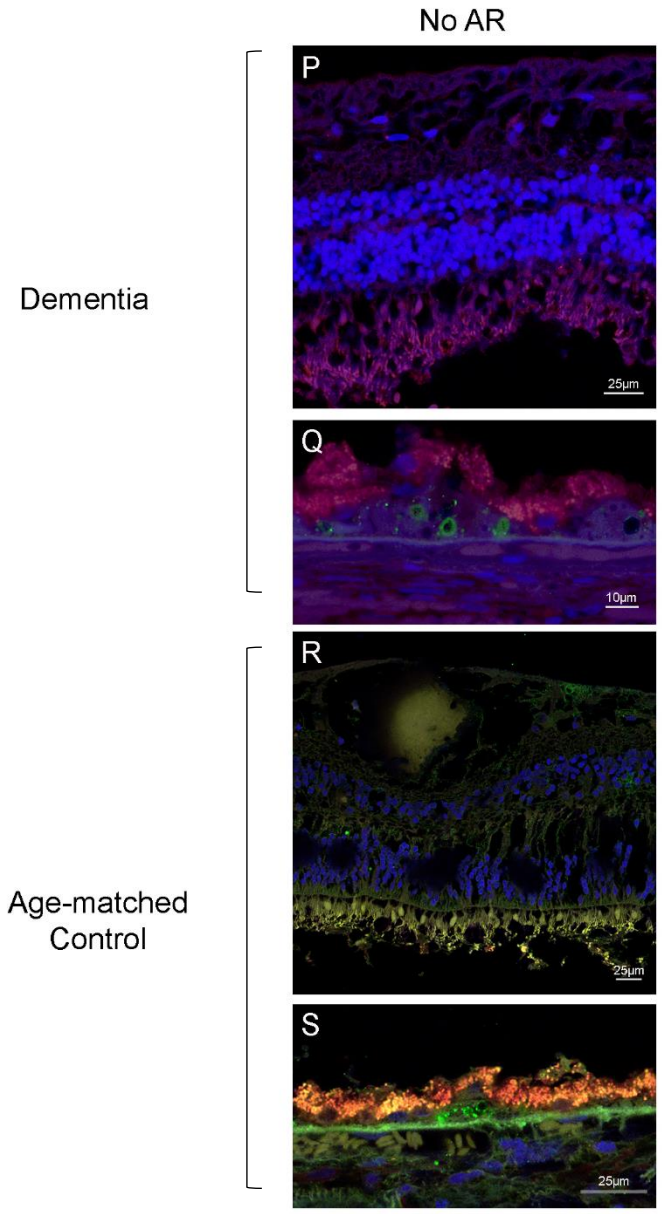

Figure 11**. Different antigen retrieval methods on cross-sections from human AD and age-matched control eyes.** Sections were stained with anti-Aβ antibody: 6E10 (green), vasculature marker: UEA-I (magenta) and DAPI for nuclei staining (blue). Comparison was made between citrate buffer retrieved (A-F), formic acid retrieved (G-O) and non-antigen retrieved samples (P-S). (A, D and E) Representative retinal images stained for Aβ with citrate buffer retrieval. Intracellular Aβ labelling detected in GCL in age-matched control sample (D and E). (G, K, M and N) Formic acid retrieval retinal images. Aβ labelling was detected in the retina (K and M). No Aβ was detected in retinal images from non-antigen retrieved samples (P and R). (B, C and F) Representative sub-RPE images stained for Aβ with citrate buffer retrieval, (I and L) formic acid retrieval and (Q and S) no antigen retrieval. Aβ labelling within drusen was detected in all samples. Sclera labelling was also present (I). Sub-RPE and retinal images of negative control samples subjected to formic acid retrieval show no Aβ labelling (J & O respectively). NFL-nerve fiber layer, GCL-ganglion cell layer, IPL-inner plexiform layer, INL-inner nuclear layer, OPL-outer plexiform layer, ONL-outer nuclear layer, PL-photoreceptor layer, RPE- retinal pigment epithelium, BM-Bruch's membrane and C-choroid.

Human - Flat-Mount Retina & Bruch's Membrane

To determine if a relationship between Aβ accumulation and retinal vasculature exists in human flat-mount retinal tissue, initially I carried out immunostaining with anti-Aβ antibody 6E10 and human vasculature lectin UEA-I. Flat-mount retina and Bruch's membrane from a healthy control individual were labelled with 6E10 and UEA-I in Figure 12. No antigen retrieval process was involved. Aβ labelling was detected in flat-mount retina; the labelling appears to be in small clusters located in proximity to the retinal blood vessels (Fig.12A-D). Due to the distinct pattern of nuclei within the retinal layers, these vascular-related Aβ accumulations appeared to be located within the inner layers of the retina such as GCL & INL. The distribution of Aβ labelling throughout the retinal tissue is shown in an image from a z-stack (Fig.12D), 6E10 labelling is detected in the midst of the tissue closely related to a retinal blood vessel. Similarly in another image from a z-stack, 6E10 labelling can be seen deep within the tissue (Fig.12E). A blood vessel can be seen adjacent to the Aβ labelling which may resemble extracellular Aβ plaque-like structures. Bruch's membrane was also labelled with 6E10, drusen can be seen labelled (Fig.12G) and a higher magnification image of a single druse is shown (Fig.12H). Small spherical structures were identified within drusen, similar to the distribution found within drusen in human eye cross-sectional samples. No Aβ labelling was detected in negative controls of retinal tissue (Fig.12F) or Bruch's membrane (Fig.12I).

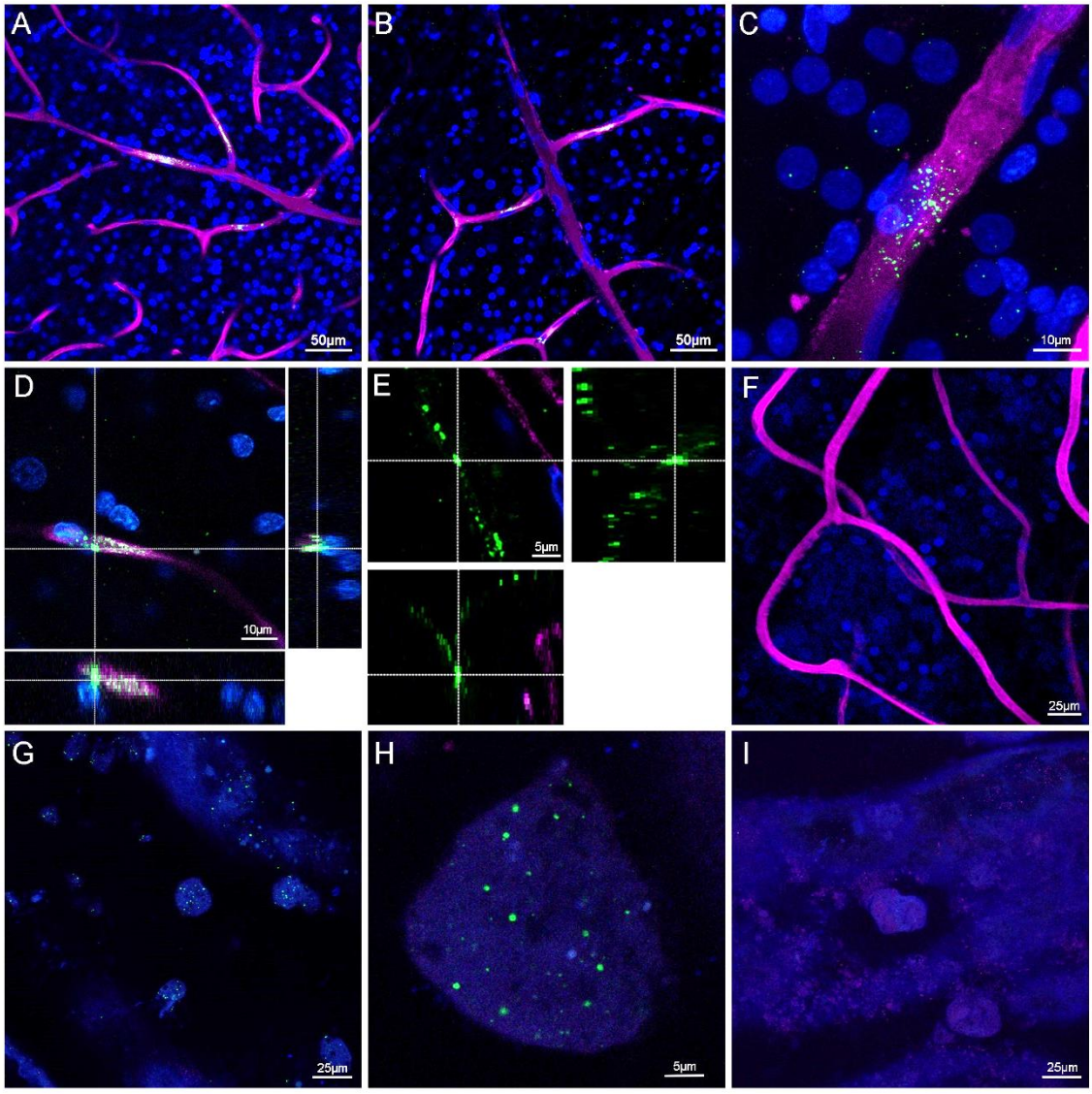

Figure 12. **Aβ labelling detected within healthy control human flat-mount retina and Bruch's membrane.** Retinal and Bruch's membrane tissue stained with anti-Aβ antibody 6E10 (green), vasculature marker UEA-I (magenta) and DAPI for nuclei staining (blue). (A & B) Representative images of Aβ labelling detected in association with retinal blood vessels. (C) Higher magnification image showing distribution of vascular-related clusters of Aβ labelling. (D and E) Images from z-stacks, sub-images to left and bottom show the depth of labelling within the tissue. (D) Aβ labelling in close proximity to retinal blood vessel. (E) A possible plaque-like Aβ labelling which appears to be in the midst of the tissue. (F) No Aβ labelling was detected in negative control sample of retina. (G) Aβ labelling detected in Bruch's membrane sample. (H) Higher magnification image of Aβ labelling within a single druse. No Aβ labelling was detected in the negative control sample (I).

To confirm if this antibody labelling was specific to Aβ, next retinal tissue was dual-labelled with another anti-Aβ antibody (CN3) (red) and 6E10 (green) in Figure 13. The retinal blood vessels and nuclei were also visualised using UEA-I (magenta) and DAPI (blue) respectively. No antigen retrieval process was involved. Aβ labelling

was detected in retinal flat-mount, similarly to previous findings the accumulations were detected in association with the vasculature within the retina. Co-localisation of 6E10 and CN3 antibodies was present within the retina (Fig.12A-D). When the separate channels for 6E10 and CN3 were analysed, the labelling of the two antibodies was similar in all cases. Correlating with previous findings, these Aβ accumulations appeared to be located within the inner layers of the retina. No Aβ labelling was detected in the negative control (Fig.12E).

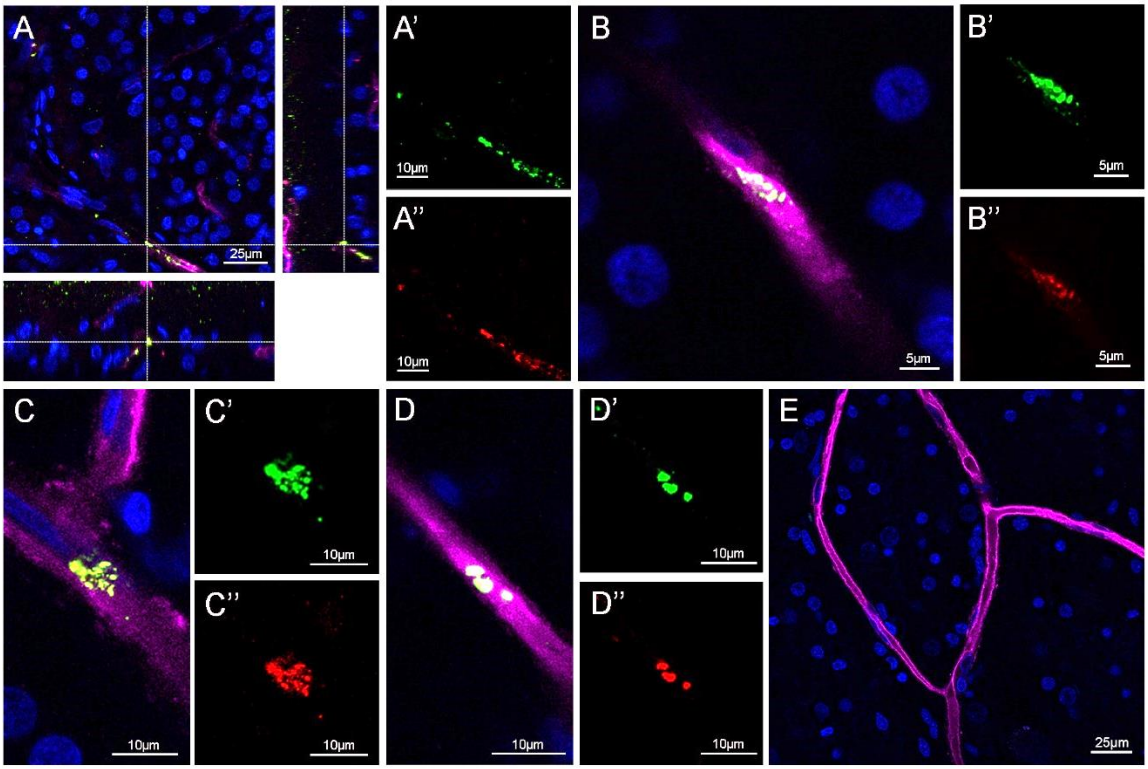

Figure 13. **Co-labelling with anti-Aβ antibodies (6E10 and CN3) on healthy control human flat-mount retina.** Tissue was stained with anti-Aβ antibodies: 6E10 (green) and CN3 (red), vasculature marker: UEA-I (magenta) and nuclei stain DAPI (blue). (A) Image from a z-stack which appears to show co-labelling of anti-Aβ antibodies in association with a blood vessel. Sub-images to left and bottom show the depth of labelling within the tissue. (B-D) Representative images of co-labelling of 6E10 and CN3 in regards to retinal vasculature. (B', C' and D') 6E10 labelling and (B'', C'' and D'') CN3 labelling. (E) No labelling was detected in the negative control.

Any Aβ labelling which was previously identified in flat-mount retina was found in non-AD samples. Therefore, the next step was to investigate how a non-AD sample would compare to an AD sample when stained for Aβ (Figure 14). Aβ (green) was detected in one single area of the AD retina (Fig.14A) and labelling was associated with a retinal blood vessel. Despite previous findings, no Aβ labelling was detected in

the age-matched control retina (Fig.14C) in this case. No 6E10 labelling was detected in the negative control samples (Fig.14B and D).

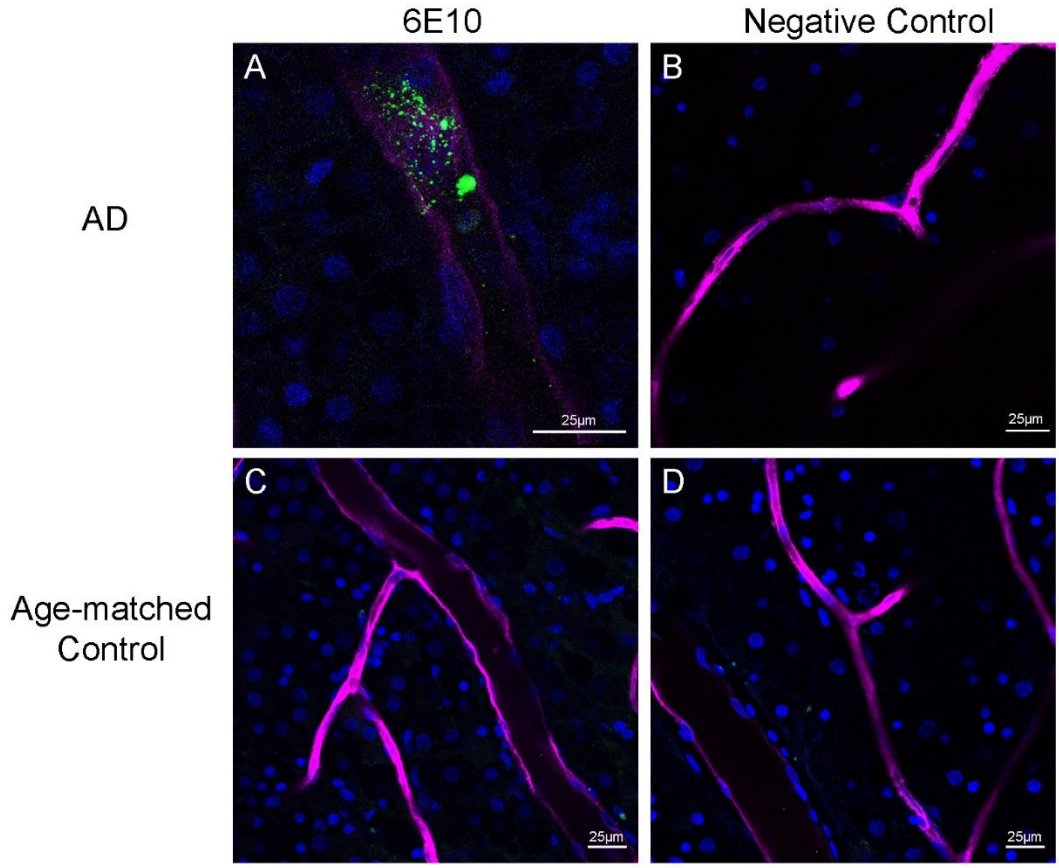

Figure 14. **Aβ staining in human flat-mount retina from AD and age-matched control samples.** Tissue was stained with anti-Aβ antibody: 6E10, vascular maker: UEA-I and DAPI for nuclei labelling. (A & C) Representative images from AD and age-matched control respectively. Vascular-related 6E10 labelling can be seen in (A) from the AD sample; however, no 6E10 labelling was detected in the age-matched control (C). (B & D) No 6E10 labelling was present in negative control samples.

Another publication which reported an increase in the amount of retinal Aβ deposits when comparing AD and age-matched control eyes was conducted by Koronyo-Hamaoui et al. (2011). They investigated flat-mount retina with curcumin and anti-Aβ antibodies. Replication of the protocol which was used in this study was carried out on AD and age-matched control retinas. AD and age-matched control retinas were stained with anti-Aβ antibody 6E10 (green) and curcumin dye (red) which labels Aβ. No Aβ plaques or deposits were found in the AD samples. There appeared to be a lot of 6E10 labelling which was on the surface of the tissue, this was not considered to be specific to Aβ. A vascular-associated 6E10 labelling was detected (Fig.15S box) in the age-matched control retina. A possible intracellular 6E10 labelling

was apparent (Fig.15A). No co-labelling was detected between 6E10 and curcumin whilst curcumin did not appear to label any Aβ-related structures within the retina. Sudan Black B (SBB) was used in order to reduce the autofluorescence in the retinal tissue. This appeared to work as the autofluorescence of melanopsin ganglion cells (arrows) and pigments (i.e. Fig.15M) in the tissue is present in samples which were not treated with SBB. No obvious differences were detected between antigen retrieved and non-antigen retrieved samples. No 6E10 or curcumin labelling was detected in negative controls.

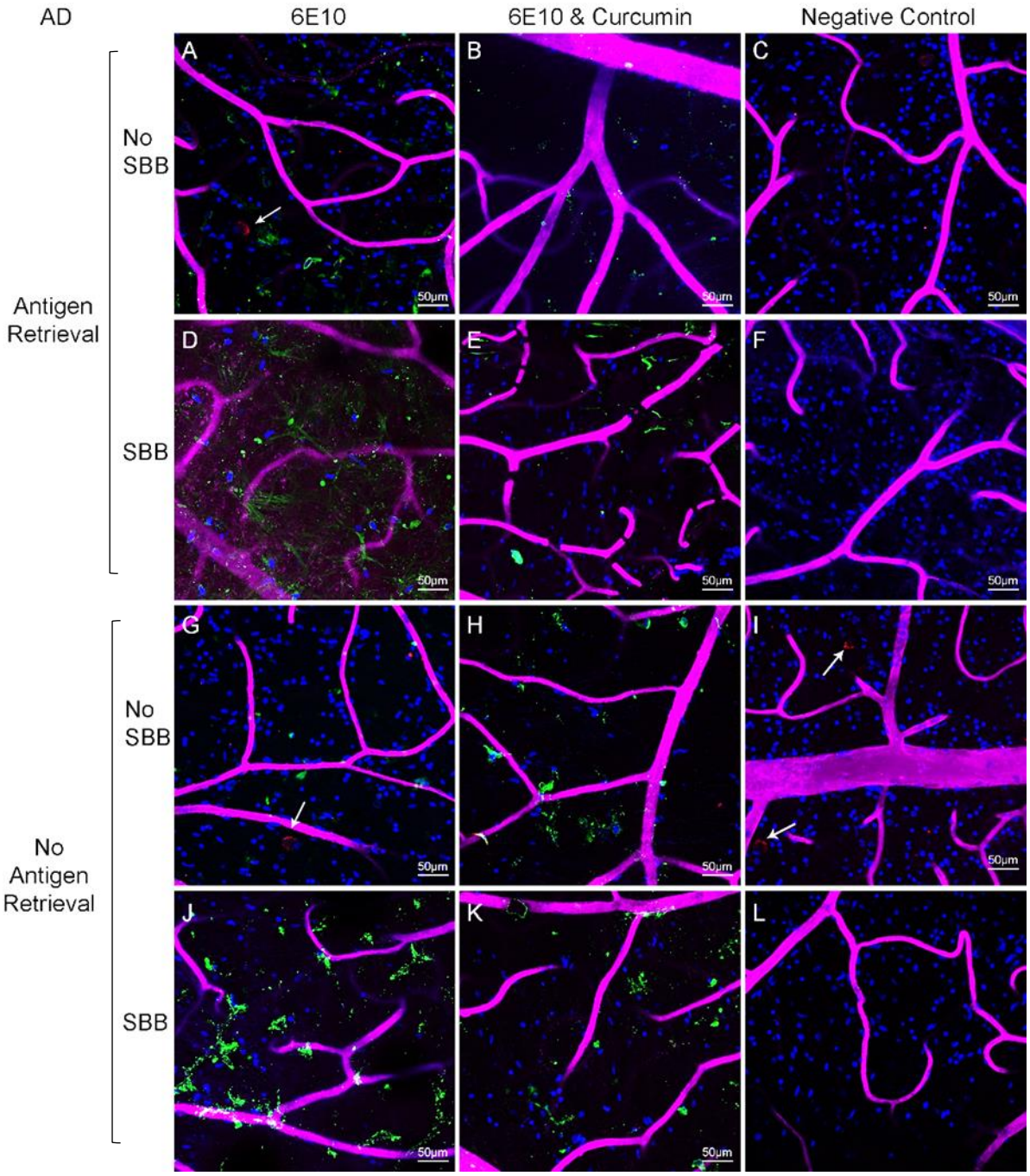

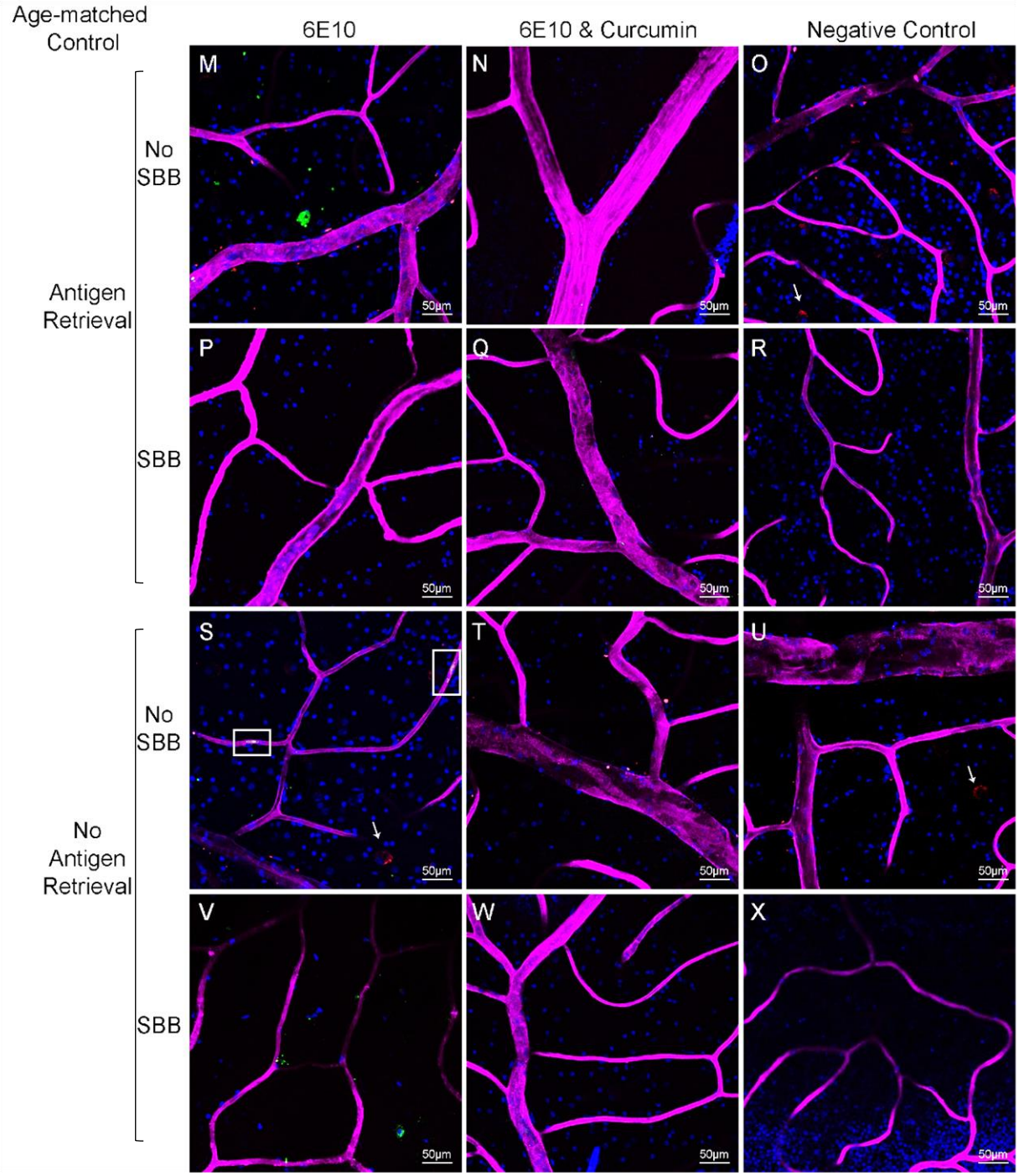

Figure 15**. Co-staining with anti-Aβ antibody 6E10 and curcumin on flat-mount retina from AD and age-matched control samples.** Comparison between antigen retrieved and non-antigen retrieved tissue was investigated and the ability of Susan Black B (SBB) dye to quench the autofluorescence. Tissue was stained with anti-Aβ antibody: 6E10 (green), curcumin (red), vascular marker: UEA-I (magenta) and nuclei stain: DAPI (blue). (A-L) Representative images from AD retina subjected to the various conditions and (M-X) images from the age-matched control retina. No Aβ plaque-like structures were detected in AD samples, the only 6E10 labelling which was deemed specific was the vessel-associated labelling seen in insets in age-matched control sample (S) and a possible intracellular labelling (A). Curcumin did not appear to label any Aβ specific structures. Red pigments which appeared individually (i.e. (M)) and within melanopsin ganglion cells (arrows) are present in tissue not subjected to SBB treatment. (C. F, I, L, O, R, U and X) Images from negative control samples.

Human - Brain Slices

Brain slices from AD and age-matched control individuals were used as a positive control to assess how retinal Aβ labelling compares to cerebral Aβ plaques. Brain slices were initially stained with 6E10 (green) and DAPI (blue) seen in Figure 16. Antigen retrieval was investigated, brain slices were subjected to heat induced citrate buffer antigen retrieval or no antigen retrieval. Aβ plaques were detected in AD (Fig.16 A and C) and age-matched control brains (Fig.16E and G). Very few plaques were detected within the age-matched control brain compared to numerous found within the AD brain. In brain slices subjected to antigen retrieval, 6E10 labelling appeared to be increased in the cerebral plaques. An intracellular Aβ labelling was also apparent in antigen retrieved samples (Fig.16A and E) but not in non-antigen retrieved samples (Fig.16C and G). No Aβ plaques were detected in any of the negative control samples (Fig.16 B, D, F and H). Brain slices were then stained with curcumin (Figure 17). Co-localisation of curcumin and 6E10 was present within brain slices of both AD and age-matched control samples (Fig.17D-F). Separate channels of 6E10 (green) and curcumin (red) labelling were analysed and the staining pattern was similar in all cases (Fig.17D'-F''). Magnified images show the morphology of cerebral Aβ plaques (Fig.17A-C and F). Autofluorescence (red) can be seen in all images. Curcumin labelling can be distinguished from autofluorescence due to the presence of co-labelling of curcumin and 6E10 (yellow).

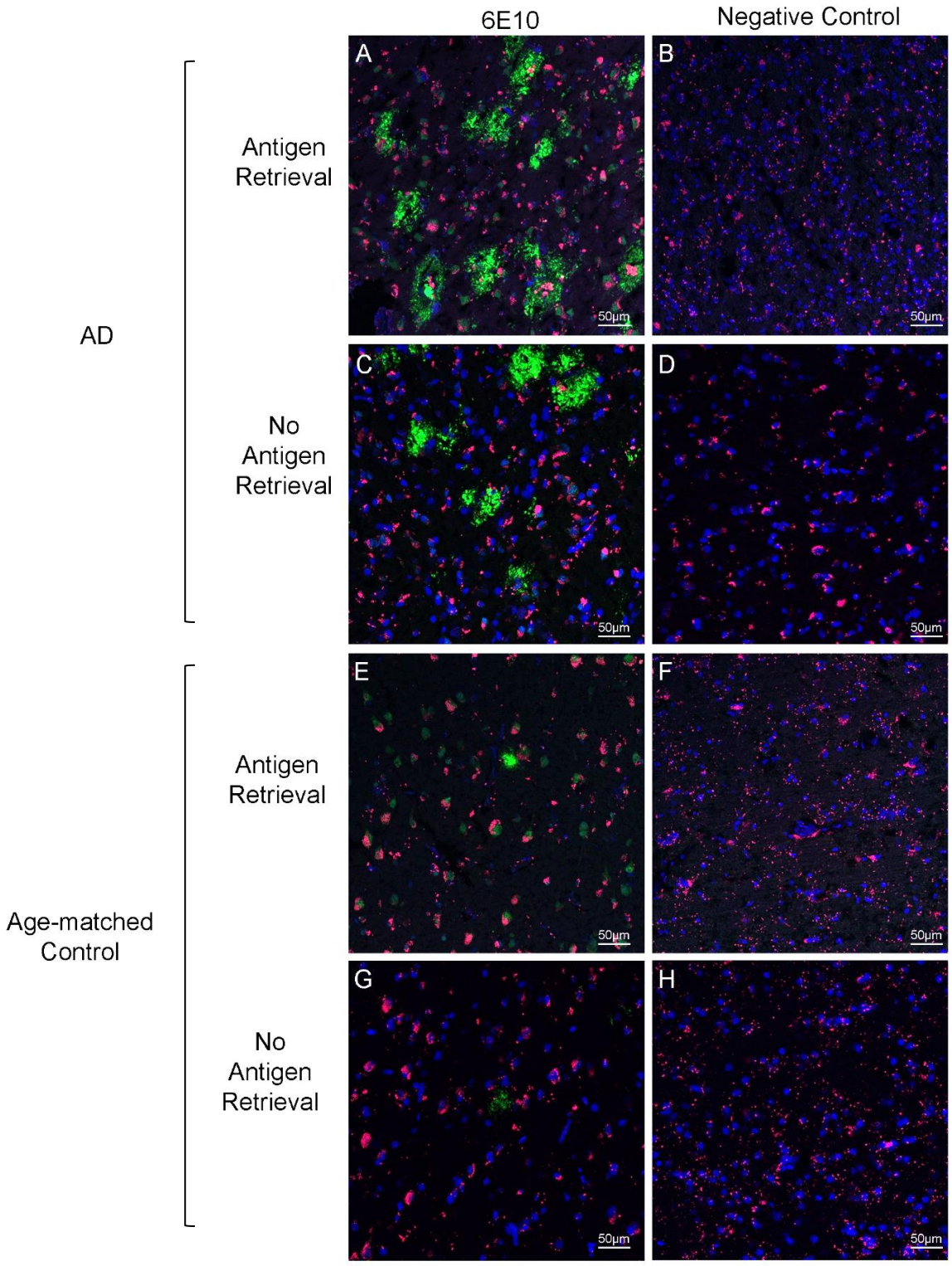

Figure 16. **Brain slices of AD and age-matched control samples labelled with anti-Aβ antibody 6E10.** Brain slices were stained with anti-Aβ antibody 6E10 (green) and DAPI (blue). Antigen retrieval was investigated. (A and C) Numerous cerebral Aβ plaques detected in the AD sample and (E and G) sparse plaques detected in the age-matched control. (A and E) A cellular 6E10 labelling apparent in antigen retrieved samples. (B, D, F and H) No 6E10 labelling detected in any of the negative control samples. Autofluorescence (red) is present.

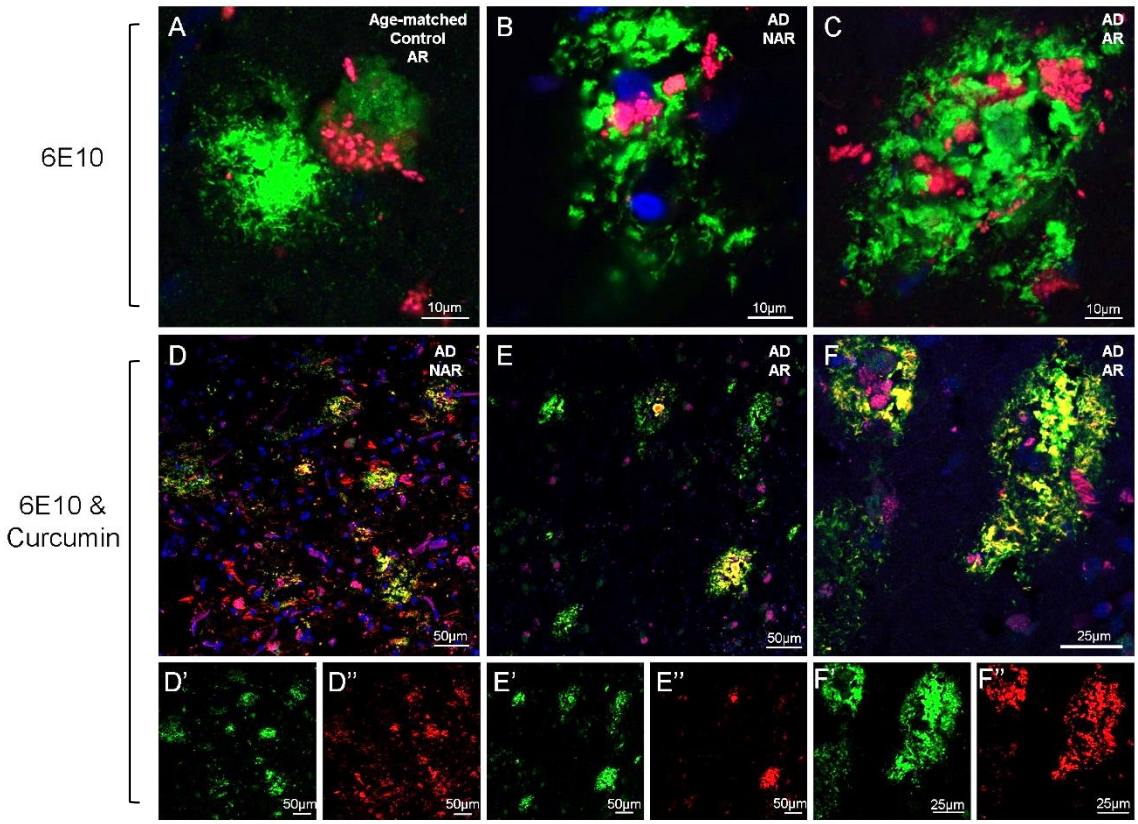

Figure 17. **Brain slices of AD and age-matched control samples labelled with anti-Aβ antibody 6E10 and curcumin.** Brain slices were stained with anti-Aβ antibody 6E10 (green) alone or co-stained with 6E10 (green) and curcumin (red) and nuclei stained with DAPI (blue). (A-C) High magnification images of 6E10 labelled Aβ plaques from age-matched control (A) and AD samples (B & C). Autofluorescence (red) can be seen within plaques. (D-F) Co-labelling of 6E10 and curcumin was detected in brain slices of AD individuals. Separate channels of 6E10 labelling (green) (D', E' and F') and curcumin (red) (D'', E'' and F''). AD-Alzheimer's disease, AR-antigen retrieval.

Transgenic Mice - Flat-Mount Retina

To visualise the retinal vasculature in mice, the best concentration of a vascular marker had to be determined. As with in human tissue, a series of different concentrations of Isolectin-B4 which labels murine vasculature were investigated. This optimisation experiment was carried out on flat-mount retina of wildtype mice. The Isolectin-B4 (magenta) concentrations used were (1:50), (1:500) and (1:1000). Nuclei was labelled with DAPI (blue). Retinal vasculature is labelled clearly with the Isolectin-B4 concentration (1:50) (Fig.18A), blood vessels can be detected with the concentration (1:100) (Fig.18B) and faint labelling can be seen with (1:500) (Fig.18C). Based on this experiment I decided to use a concentration of (1:100) for labelling the retinal vasculature in flat-mount retinal tissue and cross-sections of mice eyes.

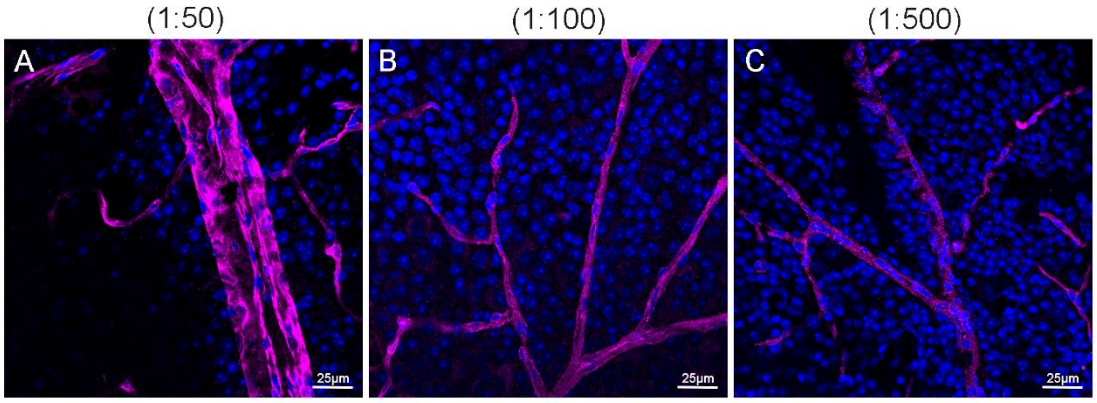

Figure 18**. Isolectin-B4 optimisation in wildtype murine flat-mount retinal tissue.** Tissue was stained with vascular marker: Isolectin-B4 (magenta) and nuclei dye: DAPI (blue). (A) Representative images of retinal vasculature from Isolectin-B4 concentrations of (1:50), (B) Isolectin-B4 concentration of (1:100) and (C) Isolectin-B4 concentration of (1:500).

To investigate the presence of retinal Aβ within the transgenic APP/PS1-21 mouse model of AD, the protocol which identified vascular-related Aβ labelling in human flat-mount retina was carried out on mice flat-mount retina. Retinal tissue from both a transgenic mouse and their wildtype littermate was stained with anti-Aβ antibody 6E10 (green) and blood vessels were visualised using vasculature marker Isolectin-B4 (magenta) (Figure 19). Mice were 9 months of age. No 6E10 labelling of Aβ plaque-like structures was present in the retinas of transgenic or wildtype mice (Fig.19A and C). No 6E10 labelling was detected in negative control samples (Fig.19B and D).

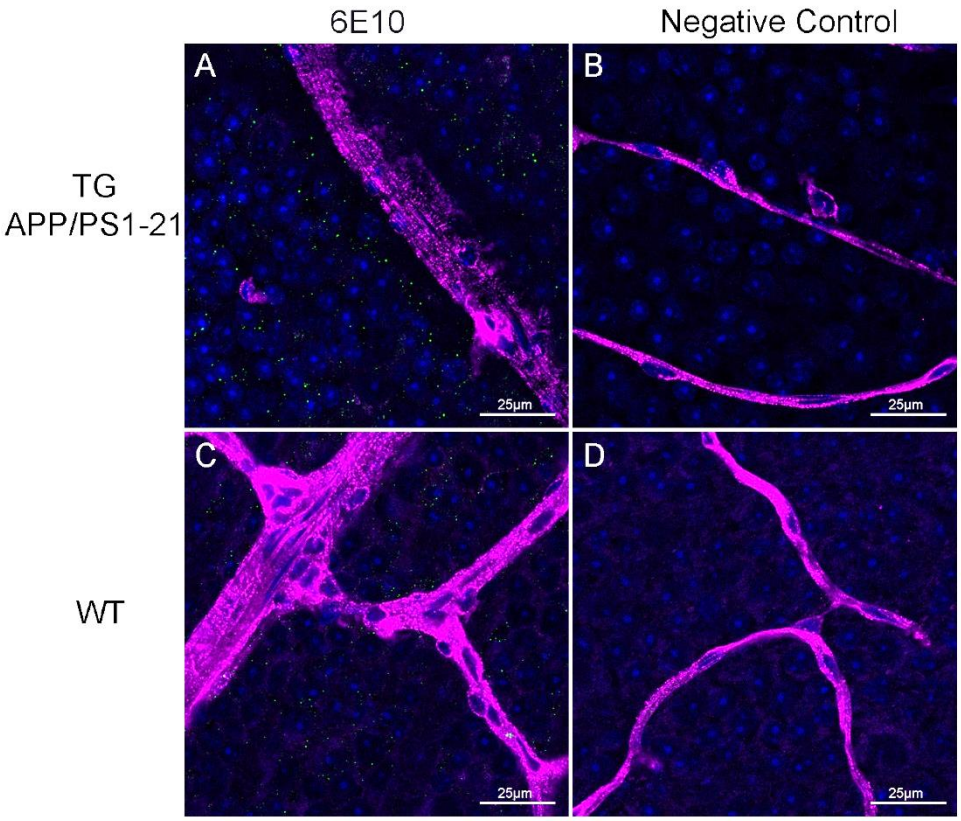

Figure 19. **Isolectin-B4 staining in transgenic (TG) APP/PS1-21 and wildtype (WT) murine retina**. Tissue was stained with anti-Aβ antibody 6E10 (green), Isolectin-B4 (magenta) and nuclei dye DAPI (blue). No specific 6E10 labelling was detected in the retina of the TG animal (A) or their WT littermate (C) or in negative controls (B & D).

No Aβ was detected in the first experiment involving transgenic mice of age 9 months, next older mice were investigated to rule out that the previous mice (Fig.19) may have been too young to develop Aβ plaques within the retina. Mice were aged 16 months and were the APP/PS1 (TASTPM) model of AD (a similar model to APP/PS1-21, with a different mutation in the PS1 gene). The same protocol which was applied on previous transgenic mice was used. Similar results were found, no retinal Aβ accumulations were detected in transgenic or wildtype mice (results not shown).

Given the success in the identification of Aβ plaques found by Koronyo-Hamaoui et al. (2011), replication of their protocol was performed in order to label retinal plaques in transgenic APP/PS1-21 mice. Mice were 9 months of age. The use of the enzyme hyaluronidase (typeI-S) was investigated. This enzyme digests any vitreous humour which may be left on the sample and may affect antibody penetration. Retinal samples were incubated with hyaluronidase (typeI-S) for either 10 or 30

minutes. Antigen retrieval was investigated. Samples were stained with anti-Aβ antibody 6E10 (green) and anti-human tau antibody (red), Isolectin-B4 (magenta) for vasculature labelling and DAPI (blue) for nuclei. Confocal microscope images were all taken in the inner retina to assess Aβ identification. No Aβ deposits were detected in any of the samples from transgenic (Fig20.A-H) or wildtype (Fig.20I-P) murine retinas. A 6E10 labelling (green) was apparent around cell nuclei in (Fig.20A). Tau was labelled densely throughout the retinal tissue, nerve fibers were labelled more brightly with the tau antibody. No obvious differences were seen in antigen retrieved and non-antigen retrieved tissue. It appeared that the use of the enzyme hyaluronidase may have been a harsh treatment as some damage was noticed on the retinal tissue. No 6E10 or tau antibody labelling was detected in negative control samples (Fig.20.B, D, F, H, J, L, N and P).

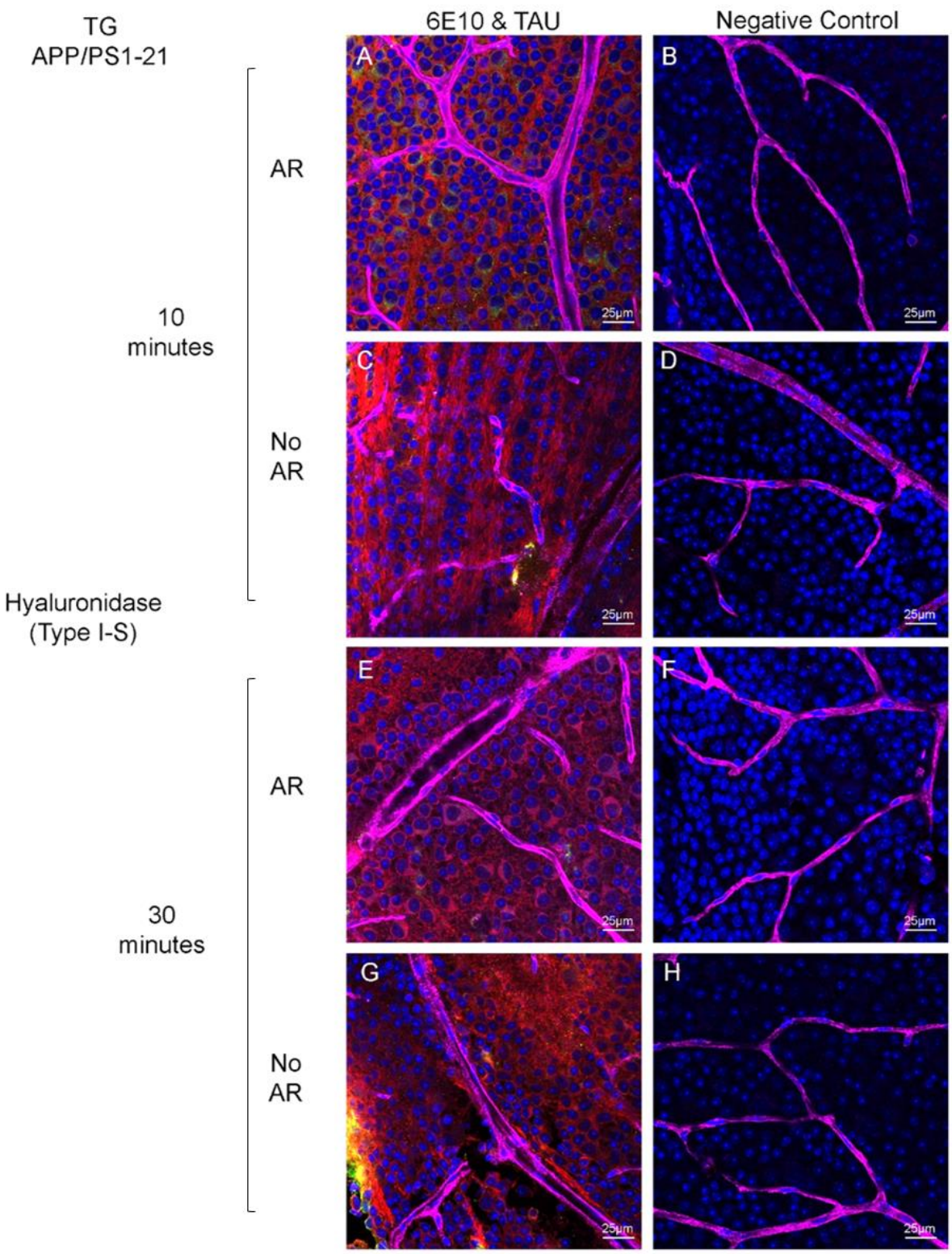
TG
APP/PS1-21
6E10 & TAU
Negative Control
AR
10
minutes
No
AR
Hyaluronidase
(Type I-S)
AR
30
minutes
No
AR
A
B
C
D
E
F
G
H
25µm

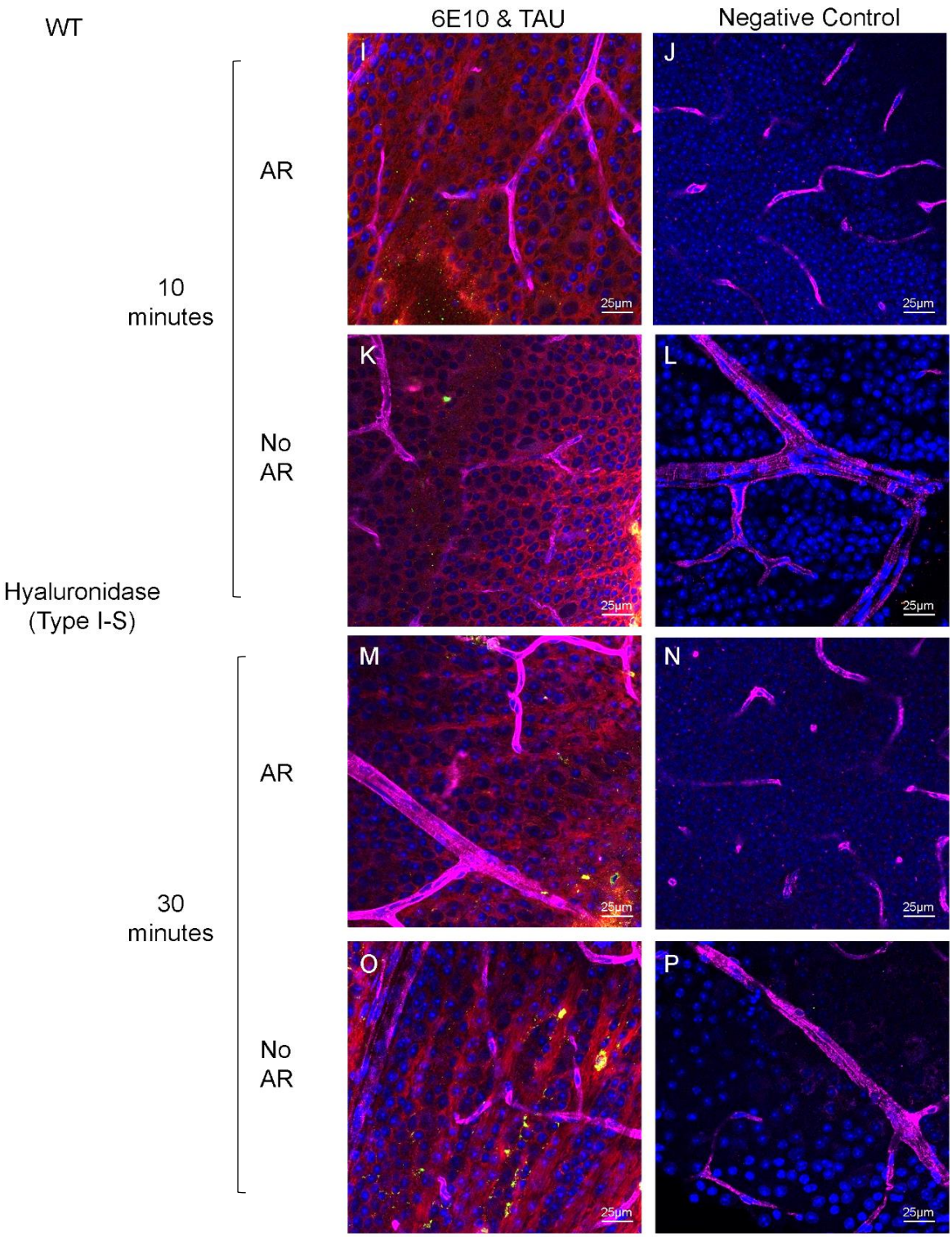

Figure 20**. Transgenic APP/PS1-21 and wildtype mice flat-mount retina stained for Aβ and tau**. Mice were 9 months old. Samples stained with anti-Aβ antibody 6E10 (green), anti-human Tau antibody (red), Isolectin-B4 (magenta) for vasculature and DAPI (blue) for nuclei. Vitreous digestion and antigen retrieval was investigated. Transgenic samples (A-H) and wildtype (I-P). 6E10 labelling was detected around cell nuclei (A). No Aβ deposits found. Tau expressed throughout the retinal tissue. TG-transgenic, WT-wildtype, AR-antigen retrieval.

I then applied the same protocol as previously used on older transgenic APP/PS1 (TASTPM) mice (Figure 21). Mice were 14-16 months of age. Samples were subjected to vitreous digestion with hyaluronidase (typeI-S) for 20 minutes or no hyaluronidase treatment. Confocal microscope images were all taken in the inner retina to assess Aβ identification. Antigen retrieval was investigated with samples subjected to antigen retrieval with modified citrate buffer or no antigen retrieval process. Similarly to the previous experiment, 6E10 labelling (green) was detected around cell nuclei (Fig.21A). No other Aβ-specific labelling was detected in any of the samples from wildtype or transgenic murine retinas. Vast expression of tau was detected in all samples treated with the tau antibody (red). Retinal vasculature (magenta) and nuclei (blue) were labelled. No 6E10 or tau antibody labelling was detected in negative control samples (Fig.21.B, D, F, H, J, L, N and P).

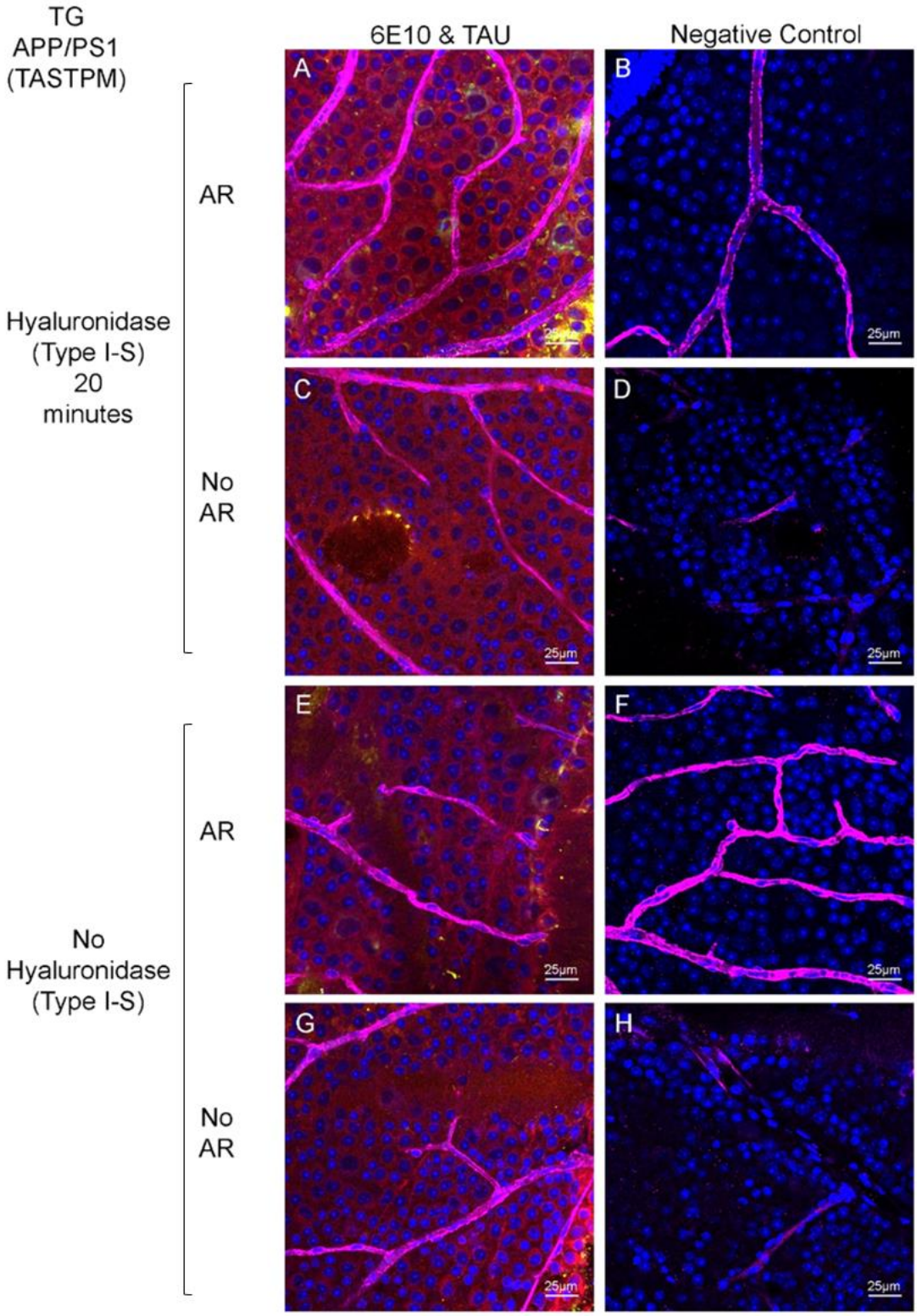
TG
APP/PS1
(TASTPM)
6E10 & TAU
Negative Control
A
B
AR
Hyaluronidase
(Type I-S)
20
minutes
C
D
No
AR
E
F
AR
No
Hyaluronidase
(Type I-S)
G
H
No
AR
25µm

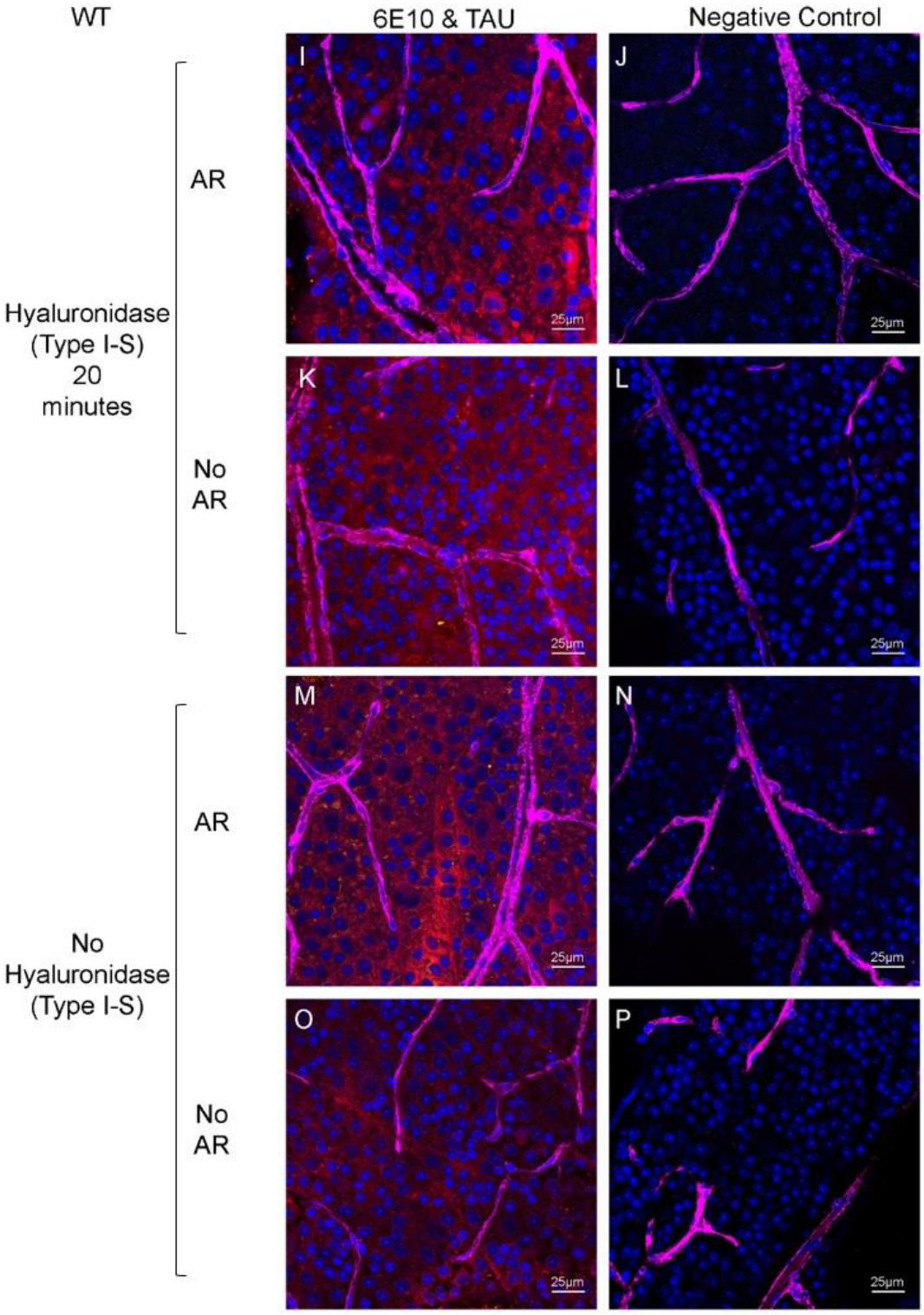

Figure 21. **Transgenic APP/PS1 (TASTPM) and wildtype mice flat-mount retina stained for Aβ and tau.** Mice were 14-16 months old. Samples stained with anti-Aβ antibody 6E10 (green), anti-human Tau antibody (red), Isolectin-B4 (magenta) for vasculature and DAPI (blue) for nuclei. Vitreous digestion and antigen retrieval was investigated. Transgenic samples (A-H) and wildtype (I-P). 6E10 labelling was detected around cell nuclei (A). No Aβ plaque-like deposits found. Tau was expressed throughout the retinal tissue. TG-transgenic, WT-wildtype, AR-antigen retrieval.

Transgenic Mice - Cross-Sections of Eyes

Approaching the end of my project, I investigated cross-sections of eyes from transgenic APP/PS1 (TASTPM) and wildtype mice. Transgenic mice were aged 25 months and wildtype mice were aged 21 months. I investigated the effect of different antigen retrieval methods, using heated citrate buffer and formic acid. One cross-section from transgenic and wildtype mice had no antigen retrieval process applied. Sections were immunostained with anti-Aβ antibody 6E10 (green) and vasculature marker Isolectin-B4 (magenta) and DAPI (blue) for nuclei labelling. No Aβ plaque-like structures were found in the retina of either transgenic or wildtype mice. An intracellular staining was detected in the GCL of the retina in the cross-section of the transgenic mouse eye which was treated with citrate buffer (Fig.22A). This was not present in the wildtype cross-section treated with citrate buffer (Fig.22B) or in formic acid or non-treated sections (Fig.22C and E). No Aβ labelling was detected in formic acid (Fig.22C and D) or non-antigen retrieved samples (Fig.22E and F). No 6E10 labelling was detected in negative control samples (Fig.22G and H). Negative controls in this case were treated with formic acid antigen retrieval and no 6E10 antibody was applied. The vascular marker did not appear to work in this experiment.

Figure 22**. Immunostaining of Aβ in cross-sections of eyes from transgenic APP/PS1 (TASTPM) and wildtype mice subjected to different antigen retrieval methods.** Cross-sections were subjected to either heated citrate buffer (A and B), formic acid (C and D) or no antigen retrieval (E and F). Sections were stained for anti-Aβ antibody 6E10 (green), Isolectin-B4 (magenta) and DAPI (blue) for nuclei. Negative controls were treated with formic acid retrieval (G and H). (A) 6E10 labelling was detected in ganglion cell layer (GCL) in a transgenic mouse eye cross-section treated with citrate buffer. No 6E10 labelling was detected in any other samples. TG-transgenic, WT-wildtype, AR-antigen retrieval. NFL-nerve fiber layer, GCL-ganglion cell layer, IPL-inner plexiform layer, INL-inner nuclear layer, OPL-outer plexiform layer, ONL-outer nuclear layer, PL-photoreceptor layer, RPE-retinal pigment epithelium and C-choroid.

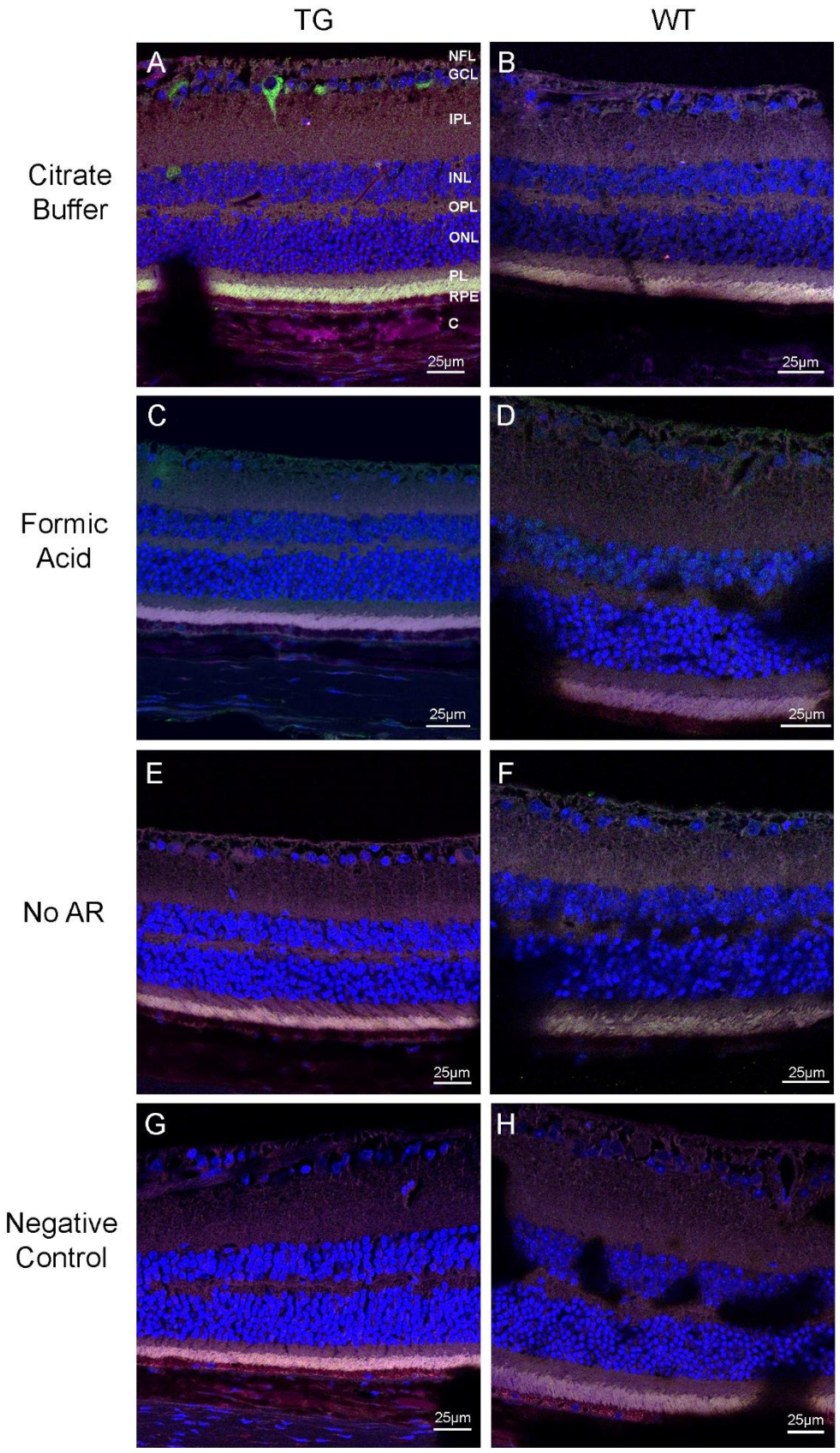
TG
WT
Citrate Buffer
Formic Acid
No AR
Negative Control
A
B
C
D
E
F
G
H
NFL
GCL
IPL
INL
OPL
ONL
PL
RPE
C
25µm

Discussion

The investigation of Alzheimer's disease-associated pathologies within the human retina is a recent area of research. In particular, retinal Aβ deposition has been investigated by few studies and inconsistent findings have been reported. My research has focused on the identification of Aβ within the retina of humans and transgenic mouse models of the AD. A large part of my research involved the optimisation of immunohistochemistry techniques. I investigated factors such as antigen retrieval methods, antibody concentrations and incubation times in order to find the most optimal conditions for Aβ immunostaining. Based on the most optimal conditions, Aβ was identified in various parts of the eye. Aβ labelling was detected in both human retinal flat-mount and cross-sectional samples and murine flat-mount retinal and cross-sectional samples. In regards to Aβ within the retina, Aβ aggregates were detected in the human retina in both AD and age-matched controls, in this case there appeared to be an association between clusters of Aβ deposits and the retinal vasculature. No increase in retinal Aβ deposits was found in AD samples when compared to age-matched control samples. An intracellular Aβ labelling was detected in the retina of both humans and transgenic mice. Aβ labelling was also detected in other areas of the eye in human dementia and age-matched control samples such as drusen, choroid and sclera.

Aβ Detection in Drusen, Choroid and Sclera

The cross-sections of the human eye used in this research were known to possess drusen deposits, which can occur naturally in the aging process (Thompson et al., 2015; Löffler et al., 1995). When these sections were immunostained with the anti-Aβ antibody 6E10, labelling was detected within drusen in a spherical like form similar to findings within previous publications (Thompson et al., 2015; Anderson et al., 2004; Luibl et al., 2006). Aβ labelling was detected in drusen in both dementia (subtype unknown) and age-matched control samples. No differences were found in Aβ labelling within drusen in dementia and age-matched control samples. The nature of the spherules within drusen appear to be diverse, some are not labelled with the Aβ antibody but appear black spherical structures (Fig.10D and Fig.11C), others which only stain for HAP (Fig.8) and some which are labelled for with both Aβ and HAP (Fig8B, C and E). Whilst some druse have no labelling at all (Fig.7K). Aβ labelling was also detected in drusen in flat-mount samples of Bruch's membrane. This labelling was in a similar pattern to the labelling identified in drusen in cross-sectional samples, small circular structures were present. Aβ labelling within drusen was detected in all

samples stained with the 6E10 antibody even if no antigen retrieval process was applied. Due to the detection of Aβ in drusen, cross-sections were often used as a positive control in experiments involving flat-mount tissue. In this case, cross-sections would be treated identical to flat-mount tissue, if Aβ was detected within drusen in cross-sections it confirmed that the 6E10 antibody worked. Aβ labelling in spherules was also detected around basal areas, within the choroid and sclera.

Comparisons between drusen and cerebral plaques in AD has shown that the two structures share similarities. They may have similar processes of formation, given they both have the ability to spontaneously aggregate Aβ. Comparisons have also been made between their contents, both structures have been shown to contain different forms of amyloid (Kayed et al., 2003, Luibl et al., 2006), have been associated with lipids (Koronyo-Hamaouri et al., 2011; Thomspon et al., 2015; Wang et al., 2010) and complement components (Yasojima et al., 1999; Johnson et al., 2001). Therefore research into Aβ deposition in drusen could potentially give an insight into the formation of cerebral plaques characteristic of AD.

Spherules within drusen have been proven to contain HAP, a calcium phosphate which is commonly found in bones and teeth. These HAP spherules may be coated with a number of different proteins including Aβ (Thompson et al., 2015). Similarly, another study reported that Aβ was associated with the outer layer of these spherules (Johnson et al., 2002). This concept may explain why a vast amount of spherules were labelled with HAP whilst only few were labelled with Aβ. It may also explain the co-labelling of HAP and Aβ obtained on individual spherules, these may be HAP spherules which are coated with Aβ. In contrast, this co-labelling was detected in the choroid and sclera in my research as opposed to within drusen which was found in the publications mentioned previously.

Aβ labelling was detected within the sclera in human cross-sectional samples. This was an unexpected finding as there is very little evidence of Aβ deposition within the sclera in published data. One study which reported scleral Aβ labelling in association with AD found deposits in the sclera of a transgenic mouse model of AD. Only few deposits were detected (Koronyo-Hamaoui et al., 2011), whereas in my findings the sclera is very densely labelled. This vast amount of Aβ labelling was detected in the sclera of human samples in both dementia (subtype unknown) and age-matched controls. Since this scleral labelling was found in both dementia and age-matched controls, it is not specifically associated with dementia or AD. When the sclera was stained with Osteosense which labels HAP; a calcium phosphate, the

sclera was also densely labelled. This would suggest that the sclera may be calcified. Given the association between HAP and Aβ within spherules in drusen, a possible link may exist between calcification of the sclera and Aβ labelling. However, the focus of my research was retinal Aβ deposition therefore this was not investigated further.

Aβ Detection within the Human Retina

Much controversy exists regarding the presence of Aβ deposits within the retina. In human flat-mount retina, labelling was detected in an AD and age-matched control sample. Aβ labelling in both cases appears to be associated with retinal blood vessels. It is difficult to establish the retinal layers when viewing flat-mount tissue; however, given the distinct nuclei distribution within the retina, it was estimated that the vascular-related Aβ labelling was located in the inner retinal layers. Vascular-related Aβ deposits were detected in the retina of a non-AD individual; however, any retinal tissue which was labelled was from one individual. This finding was not surprising as sparse Aβ deposits have been found in the retina of healthy eyes by other studies (La Morgia et al., 2016; Koronyo et al., 2017). Few Aβ plaques were also found in the brain of healthy individuals which supports that existence that low levels of Aβ deposits may be present within the retina and brain of healthy individuals.

In regards to vascular-associated Aβ labelling in the retina of individuals with AD, this was only present on one account where few deposits were located in a single area of the retina. Much larger quantities of Aβ deposits would have been expected in an AD sample if retinal deposition correlated with cerebral deposition. Although similarly to the vascular-related Aβ labelling in non-AD samples, any AD retinal flat-mount tissue was from a single individual. Results may have differed if more AD samples were analysed.

I investigated co-staining of two anti-Aβ antibodies (6E10 and CN3) in a non-AD sample. Co-localisation of the antibodies was present in various areas of the retinal tissue. This provided confirmation that the labelling was specific to Aβ-related structures. However, samples were also co-stained with anti-Aβ antibody 6E10 and curcumin, which is a dye which binds Aβ (Garcia-Alloza et al., 2007). During this experiment, sparse 6E10 labelling was detected in vascular-related areas whilst no curcumin labelling was detected in any of the samples. The vascular-related Aβ labelling with the 6E10 antibody was detected in the age-matched control sample but no Aβ deposits were identified in the AD sample. However, co-localisation of the 6E10 antibody and curcumin on retinal Aβ deposits has been detected by other studies (Koronyo-Hamaoi et al., 2011; Koronyo et al., 2017).

Aβ deposits have been found associated with the retinal vasculature by other studies. One study identified Aβ plaques in clusters which is similar to the distribution in my results. They reported abluminal Aβ deposits being the most frequently found in AD retinas (La Morgia et al., 2016). Similarly, another study found retinal Aβ plaques associated with retinal vasculature particularly in the abluminal position but plaques were also detected within blood vessels (Koronyo-Hamaoui et al., 2011). A recent study also found Aβ deposits located nearby and inside blood vessels as well as along the vessel walls. Again in a similar distribution to my findings, deposits can be seen in clusters associated with the vasculature (Koronyo et al., 2017). The vascular-related Aβ deposits which were found in my results were located in close proximity to retinal vasculature; however, I was not able to distinguish if they were located on the outside or within retinal blood vessels. The non-AD individual which presented vascular-associated Aβ deposits died from cardiovascular disease, this provides further evidence supporting a vascular disease component in AD. Vascular-associated Aβ deposits may be responsible for the changes in vasculature and blood flow which are apparent in the retina during AD (Berisha et al., 2007; Frost et al., 2013; Williams et al., 2015). The retinal vasculature and cerebral vasculature are directly linked and share anatomical and physiological similarities (Patton et al., 2005). In addition to this, vascular-related Aβ deposition identified within the retina reflects a process which occurs in the brain when Aβ is deposited in the cerebral blood vessels in the condition cerebral amyloid angiopathy. This condition is commonly found in association with AD (Thal et al., 2008) and suggests a further link between the vascular Aβ deposition in the retina and brain in AD.

Results on Aβ deposition in the retina in cross-sectional samples is minimal. Research on cross-sections involved mostly healthy control eyes, with one dementia sample being analysed. The subtype of dementia was unknown, it is possible that this samples was not AD and hence lacked Aβ pathology. Analysis of healthy control eyes allowed for the optimisation of Aβ detection within drusen and after optimisation was intended to be transferred to AD tissues. Aβ plaques were not expected to be present in the retina of healthy control eyes. Despite this, retinas were analysed due to the identification of retinal Aβ deposits in healthy control retinas on rare occurrences. A possible vascular-related Aβ deposition was detected in one area of the retina in a cross-section of a healthy control eye which was subjected to formic acid retrieval. The lack of definite AD cross-sectional samples analysed is likely to be responsible for the shortage of retinal Aβ deposits identified.

An intracellular Aβ labelling was detected in the GCL in cross-sections of the eye. This Aβ labelling was apparent in cross-sections which were treated with heat induced citrate buffer antigen retrieval. However, the cross-sections which exhibited intracellular ganglion cell labelling were from a single non-AD sample and this labelling was not present in other non-AD samples which were treated identically. A study by La Morgia et al. (2016) reported that a subtype of ganglion cells; melanopsin ganglion cells exhibit Aβ immunoreactivity. Melanopsin ganglion cells may exhibit Aβ labelling but they also express autofluorescent red pigments when viewed under confocal microscope. The ganglion cell labelling most often detected in my results was a more intense Aβ labelling and no red pigments were expressed. Therefore I believe the ganglion cells detected in my results which were labelled intracellularly for Aβ are distinct from melanopsin ganglion cells. Likewise, a cellular labelling was also detected in flat-mount retinal tissue which was subjected to citrate buffer retrieval process. This appeared to be in the inner layers of the retina therefore could possibly have been located in the GCL. A possible cellular or vascular-related labelling was detected in the cross-section of a non-AD eye which was subjected to formic acid retrieval; however, this was only apparent in a single area of the retina and is distinct from the numerous ganglion cells which appear labelled in the citrate buffer treated samples. Intracellular Aβ is not well characterised within the human retina, although a similar intracellular Aβ immunoreactivity was detected in the GCL in AD retinal samples using the 6E10 antibody by another study (Koronyo et al., 2017). Intracellular Aβ was also detected with an antibody specific to Aβ42 (12F4), the study concluded that intracellular Aβ could be an alternative method of Aβ-medicated toxicity. Intracellular labelling was also detected by Koronyo-Hamaoui et al. (2011) in AD post-mortem retina, it was suggested that this was Aβ40 as the antibody used was specific to this Aβ peptide (11A5-B10).

The replication of two different protocols from experimental studies which reported the identification of Aβ deposits in the human retina (La Morgia et al., 2016; Koronyo-Hamaoui et al., 2011) did not prove successful in identifying Aβ deposits.

I analysed the retinas from 1 AD, 1 dementia (subtype unknown) and 5 control samples. The AD sample was flat-mount retina and the dementia sample was a cross-section of the eye. Retinal Aβ deposits were found in many areas in a control sample and in one area in an AD sample. In all cases where Aβ deposition within the retina was detected, a retinal blood vessel was located nearby. This suggests a link between Aβ deposition and the retinal vasculature. As previously mentioned, the lack of retinal Aβ deposits located in relation to AD is likely to be due to the low number of definite

AD samples analysed. A larger number of AD samples would need to be used to determine of retinal Aβ deposition is a pathology associated with AD.

Aβ Detection within the Human Brain

Brain slices were used as a positive control in order to compare retinal Aβ deposition with cerebral Aβ plaques. Cerebral plaques were much larger in size than any retinal deposits which were identified. Plaques within the brain were more numerous in the AD sample than Aβ deposits which were found in the retina of the AD eye. When brain slices were co-labelled with 6E10 and curcumin, co-localisation was present in Aβ plaques; however, this did not occur when the AD retina was labelled with 6E10 and curcumin as previously mentioned. This suggests that differences exist in the composition of cerebral plaques and retinal deposits consisting of Aβ. A clear difference was seen in the brain pathology between the AD and age-matched control sample. A large number of plaques were detected in the AD brain whilst few were detected in the age-matched control. This is contrasting to the retina where no increase in Aβ deposits was detected in AD when compared to age-matched control samples. Few plaques were detected in the age-matched control brain which supports the idea that cerebral Aβ plaques precede cognitive decline in AD (Price et al., 2009). An intracellular labelling was also detected in the brain of AD and age-matched control samples which were subjected to citrate buffer antigen retrieval, this labelling was similar to what was found in the GCL of human retinal samples. It is possible that this intracellular labelling could be due to antibody cross-reactivity as it appears the epitope which is recognised by the 6E10 antibody is present on both Aβ and its precursor protein APP. Evidence of this is shown by an experimental group who detected a cellular labelling within the brain. When 6E10 labelling was compared with an antibody specific to APP, a similar staining pattern was observed. The intracellular 6E10 labelling appeared to be APP and not Aβ (Aho et al., 2010). Despite this, intracellular Aβ in regards to AD has been described. The presence of cellular Aβ is better characterised within the brain in regards to AD than within the retina. Intracellular Aβ within neurones of the brain is thought to contribute to disease progression (LaFerla et al., 2007). The neurotoxic Aβ42 peptide was detected inside cell bodies in the brain in a study by Ohyagi et al. (2007). Interestingly, this research compared antigen retrieval with heated citrate buffer and formic acid. Aβ was detected within cells with the citrate buffer retrieval whilst no cellular labelling was seen using formic acid retrieval, these findings within the brain were similar to results I found within the retina. Furthermore, intracellular Aβ has been proposed to occur prior to and may give rise to cerebral plaques in AD (Oddo et al., 2006; Pensalfini et al., 2014).

The pathogenic nature of intracellular Aβ has been characterised in the AD brain; however, the intracellular nature of Aβ within the retina needs to be further investigated to determine if it is related to AD pathogenesis.

Aβ Detection in Transgenic Mouse Models of AD

The presence of Aβ within the retina of transgenic animal models of AD has more consistent findings in publications than the presence of Aβ in the human retina in AD. Despite this, I was unable to detect any Aβ deposits within the retina of transgenic mouse models of AD. The only Aβ-related labelling detected with the 6E10 antibody was intracellular, within the inner layers of the retina in flat-mount tissue and located in the GCL in cross-sections. The 6E10 labelling in the cross-section of an eye from a transgenic mouse was detected in a section which was subjected to heat induced citrate buffer antigen retrieval. This was similar to the intracellular labelling within human retinal tissue which was also more apparent with this method of antigen retrieval. The Aβ labelling in the cross-section shows typical ganglion cell morphology with dendrites extending into the inner plexiform layer. A similar staining pattern was detected in another study on a transgenic mouse model of AD although the labelling in this case was for the Aβ precursor protein APP (Ning et al., 2008). As previously mentioned, the 6E10 antibody labels APP as well as Aβ therefore it is possible that the labelling in my murine cross-section may be APP and not Aβ.

Plaques have been observed in the retina of transgenic mouse models of AD in a number of studies (Koronyo-Hamaoui et al., 2011; Ning et al., 2008; Perez et al., 2009; Liu et al., 2009; Tsai et al., 2014; Gupta et al., 2016). After failing to detect any plaques in my initial experiment using 9 month old transgenic mice, I investigated age as a factor which may have prevented the identification of retinal Aβ deposits. After performing the same protocol on older 16 month old transgenic mice, similarly no Aβ deposits were found. Furthermore, Aβ plaques were identified in the retina of mice as young as 2.5 months old in a similar model of AD (Koronyo-Hamaoui et al., 2011). Therefore age could not be responsible for the lack of retinal Aβ deposits detected.

After failing to detect any Aβ deposits in the retina of transgenic mice using methods which detected vascular-associated retinal Aβ in human tissue, I replicated a protocol from a publication which reported the identification of retinal Aβ deposits in transgenic mice (Koronyo-Hamaoui et al., 2011). Similar to results in the replication experiments in human tissue, the replication of the protocol in transgenic mice failed to produce successful results in Aβ deposition.

I analysed the retinas from 5 different transgenic mice and their wildtype littermates of various ages, 4 were flat-mount retinal tissue and 1 was cross-sections of the eye. In order to establish what was responsible for the lack of retinal Aβ deposits in transgenic mice, more samples would need to be investigated and alterations made to the immunolabelling protocol. The length of my research project did not allow for further investigation. Due to the lack of retinal Aβ deposits found in transgenic mouse models of AD I could not investigate the relationship between retinal vasculature and Aβ deposits.

To summarise my research, Aβ labelling was detected in regions of the retina in both flat-mount and cross-sectional samples of the eye. Where extracellular Aβ labelling was detected, in all cases there was a retinal blood vessel in close proximity suggesting a link between Aβ deposition and retinal vasculature. Vascular-related Aβ deposits were identified in the human retina in both AD and age-matched control samples. These deposits were much smaller in size than cerebral Aβ plaques. No increase in Aβ deposits were found in AD samples when compared to age-matched controls. A complete lack of Aβ deposits were found in the retina of transgenic mouse models of AD. Aβ was detected in the sub-RPE region including drusen, choroid and sclera although no difference was found between dementia samples and age-matched controls. An intracellular Aβ labelling was detected in human retina, brain and transgenic mouse retina. This appears to be associated with antigen retrieval with citrate buffer and was only apparent after an antigen retrieval incubation time of 9 mins or greater. There is a possibility that this labelling is APP and not Aβ due to the same epitopes in Aβ and APP. However, intracellular Aβ is apparent in the brain during AD (Pensalfini et al., 2014), therefore this concept occurring within the retina should not be ruled out until further clarification is obtained.

Limitations of My Research

Immunohistochemistry is a technique which allows identification of proteins of interest. Identification of Aβ was possible; however, no quantitative data analysis was included in my research project. The ability to determine how much Aβ peptide was present in key areas of interest such as vascular-related sites of identification and intracellular Aβ labelling or how many areas of Aβ deposition occurred in a single retina would have provided more information on the nature of retinal Aβ.

Three different agents specific to Aβ were used: anti-Aβ antibodies 6E10 and CN3 and the dye curcumin. The antibodies were specific to the same region on the Aβ peptide; the N-terminus. These antibodies are unable to distinguish between APP

and different forms of the Aβ peptide such as Aβ40 or Aβ42. The use of other antibodies which recognise different epitopes on the Aβ peptide and be able to distinguish between Aβ peptides and precursor proteins would have provided more conclusive results. Curcumin was able to detect cerebral Aβ plaques but no labelling was found in the retina. Curcumin labelled Aβ plaques within the retina have been described (Koronyo-Hamaoui et al., 2011; Koronyo et al., 2017); however, I only investigated curcumin in one experiment so replication may have been needed.

The antigen retrieval method mainly used in my research was heated citrate buffer. Antigen retrieval by formic acid is the method routinely described in the literature in regards to retinal Aβ identification (Ning et al., 2008; Liu et al., 2009; Dutescu et al., 2009). I only investigated formic acid as a method of antigen retrieval for detection of Aβ in one experiment in human and mice. However, other methods of retrieval have been reported successful in retinal plaque detection as Koronyo-Hamaoui et al. (2011) report Aβ plaques with citrate buffer retrieval. I used citrate buffer in the majority of my research as detection of Aβ aggregates within drusen was possible with this antigen retrieval method. Although, it is a possibility that differing forms of Aβ exist in drusen and retinal Aβ deposits and this may be responsible for the lack of retinal deposits detected in many cases.

Where Aβ labelling was detected in flat-mount tissue, it was often in very few areas. Therefore when analysing cross-sections, key pathologies could have be missed due to sectioning of the eye. Sectioning a whole eye and immunostaining it would have produced more conclusive results in distinguishing the presence of Aβ deposition.

Difficulties were experienced in the identification of retinal Aβ deposition in relation to AD therefore the protocols from two experiments studies which reported successful findings were replicated. However, the replication of these protocols was only possible to a certain extent. The protocols which were carried out on human tissue did not result in Aβ plaque-like structures being detected. Although some conditions differed between my research and the original research, these included the replication protocol which was carried out on cross-sections in my research was carried out on flat-mount retinal tissue in the original experimental study (La Morgia et al., 2016). Furthermore my analysis was on individuals who were not diagnosed with AD. In the experimental study by Koronyo-Hamaoui et al. (2011), the hyaluronidase treatment was used on human tissue to digest the vitreous whilst this treatment was not used in my experiments on human retina. This study also

investigated a number of different agents in the detection of Aβ whilst I only used the 6E10 antibody and curcumin. I also replicated the protocol used on transgenic mice in the publication by Koronyo-Hamaoui et al. (2011). Despite the vast amount of retinal deposits found in this publication, no Aβ plaque-like structures were located in the retina of transgenic mice in my research. Hyaluronidase treatment was used to digest any remaining vitreous residue, in the original research this was performed on fresh tissue whilst I did not have access to fresh tissue therefore fixed tissue was used instead. A variety of different agents were used to label retinal Aβ in this research whilst I only used the 6E10 antibody. It is possible that these conditions may account for the lack of deposits found in these experiments.

In terms of samples used, few AD samples were used in my research. The vascular-related Aβ labelling in both AD and age-matched control flat-mount retinal tissue were from a single patient in each case. Only one AD retinal flat-mount sample was used and cross-sections from one dementia sample of which the subtype was unknown. This sample may not have been AD therefore may explain why no retinal Aβ accumulations were identified in human cross-sections. A larger sample size would have provided more reliable results although the difficulties in obtaining human tissue must be considered.

Furthermore, not all the information for the samples used was available. No information was available for the post-mortem time of the human samples, this may cause degeneration of the tissue and affect the ability to identify Aβ. No information was given on the stage of AD or the length of time in which an individual had the condition, there would be different degrees of pathology with progression of AD and this may affect the amount of Aβ deposits present in the retina. Finally, the cause of death for many of the samples was not available. This would have been useful in providing more information on the medical history of the patient samples used.

One AD brain sample was included in my research as a positive control in order to assess how cerebral Aβ plaques appear when immunolabelled and how they compare to retinal Aβ deposits. I did not investigate if Aβ plaques were associated with the cerebral vasculature, it would have been interesting to explore if cerebral Aβ plaques were associated with vasculature in a similar way to the vascular-related Aβ deposits which were detected in the retina. The brain which was investigated was not from any of the samples in which retina was explored. Ideally it would have been better to have the eye and brain of the same individual or transgenic animal to

evaluate the comparison of Aβ load within the brain and retina. This would have been a true indicator if retinal pathology could be representative of brain pathology in AD.

I only investigated Aβ accumulation within the retina in association with AD. It would have been interesting to evaluate another AD-associated pathology such as NFT's. Although I did explore the expression of tau within retinal tissue, immunolabelling for phosphorylated tau would have provided more insight into AD-associated changes within the retina.

Conflicting Results in Published Data

Inconsistent results have been reported in the literature in regards to Aβ within the human retina. The differing results may be due to a variety of factors. Different immunohistochemistry techniques would account for different results. Antigen retrieval methods have different degrees in which epitopes are unmasked, therefore certain methods would be better for identifying particular proteins. The state of the tissue would affect results, whether fixed or fresh tissue or if cross-sections are frozen or embedded in paraffin. Furthermore, differing results may be found in flat-mount retinal tissue and cross-sections of the eye. Flat-mount tissue appears to be a more reliable indicator of tissue pathology than cross-sections where pathology could potentially be missed. Immunohistochemistry techniques would need to be altered for tissue type as flat-mount tissue tends to be thicker than cross-sections which may affect antibody penetration. Interestingly, both experimental studies which failed to detect Aβ in the human AD retina only analysed cross-sections of the eye (Schön et al., 2012; Ho et al., 2014). Whereas research studies which successfully identified Aβ deposits analysed flat-mount retinal tissue, aside from one study by Koronyo et al. (2017) which detected Aβ plaques in cross-sections of the eye and flat-mount retinal tissue (Koronyo-Hamaoui et al., 2011; La Morgia et al., 2016; Koronyo et al., 2017; Tsai et al., 2014). Therefore, flat-mount retinal tissue appears to produce more conclusive results in the detection of Aβ within the retina during AD.

Conclusion and Future Research

I detected Aβ labelling in the retina of human and transgenic mouse models of AD. An intracellular labelling was detected in human and transgenic animal samples. Aβ labelling which appears as plaque-like structures was identified in the retinas of both AD and age-matched control samples, in all cases these appeared as clusters of deposits associated with retinal vasculature. However, no increase in deposits was detected in AD samples when compared to age-matched control samples. A lack of

Aβ plaque-like structures were identified in the retina of transgenic mice. Therefore I could not investigate how the relationship between retinal blood vessels and Aβ detection in the transgenic mouse retina. Given these results, it is not possible to conclude that retinal pathology could represent brain pathology in AD.

Based on the results I obtained, future research needs to be carried out on the relevance of Aβ within the sclera of the eye. Intracellular Aβ within the retina; in particular the GCL, needs to be investigated to determine if this contributes to the pathogenesis of AD. Finally, more research into the detection of AD-associated pathologies in the retina of human AD patients is needed. To achieve this, research should ideally include comparison of brain and retina from the same individuals, larger samples of AD patients, focusing particularly on flat-mount retinal tissue and using a variety of different agents to label pathologies.

Currently, the presence of retinal Aβ plaques remains ambiguous. Despite the lack of retinal deposits identified in association with AD, I believe the retina should not yet be ruled out as representing brain pathology in AD. The retina has advantages over the brain as it can be easily accessed and viewed non-invasively. There is evidence to suggest that retinal Aβ deposits could be characteristic of cerebral plaques in AD although further clarification is needed. The diagnosis and monitoring of AD has posed challenging and therapeutic options for the condition are limited therefore new concepts need to be explored. The detection of AD-associated pathologies in the retina has the potential to provide an answer to clinical problems; however, more in-depth research comparing retina and brain is necessary.

Acknowledgements

I would first like to thank my supervisor Dr. Imre Lengyel for the opportunity to join his research group, involving me in this interesting area of research and for his advice and guidance throughout my project. I would also like to thank Lajos Csincsik and Eszter Emri for providing a welcoming and encouraging atmosphere to study and for all their help and assistance during my time in the laboratory.

References

AHO, L., PIKKARAINEN, M., HILTUNEN, M., LEINONEN, V. and ALAFUZOFF, I., 2010. Immunohistochemical visualization of amyloid-beta protein precursor and amyloid-beta in extra- and intracellular compartments in the human brain. *Journal of Alzheimer's disease: JAD,* **20**(4), pp. 1015-1028.

AKIYAMA, H., BARGER, S., BARNUM, S., BRADT, B., BAUER, J., COLE, G.M., COOPER, N.R., EIKELENBOOM, P., EMMERLING, M., FIEBICH, B.L., FINCH, C.E., FRAUTSCHY, S., GRIFFIN, W.S., HAMPEL, H., HULL, M., LANDRETH, G., LUE, L., MRAK, R., MACKENZIE, I.R., MCGEER, P.L., O'BANION, M.K., PACHTER, J., PASINETTI, G., PLATA-SALAMAN, C., ROGERS, J., RYDEL, R., SHEN, Y., STREIT, W., STROHMEYER, R., TOOYOMA, I., VAN MUISWINKEL, F.L., VEERHUIS, R., WALKER, D., WEBSTER, S., WEGRZYNIAK, B., WENK, G. and WYSS-CORAY, T., 2000. Inflammation and Alzheimer's disease. *Neurobiology of aging,* **21**(3), pp. 383-421.

ANDERSON, D.H., TALAGA, K.C., RIVEST, A.J., BARRON, E., HAGEMAN, G.S. and JOHNSON, L.V., 2004. Characterization of beta amyloid assemblies in drusen: the deposits associated with aging and age-related macular degeneration. *Experimental eye research,* **78**(2), pp. 243-256.

ANIMATED DISSECTION OF ANATOMY FOR MEDICINE (A.D.A.M.), 2017-last update, *Alzheimer's disease.* [Online]. Available: https://medlineplus.gov/ency/imagepages/8681.htm [Accessed 14 Aug. 2017].

BERISHA, F., FEKE, G.T., TREMPE, C.L., MCMEEL, J.W. and SCHEPENS, C.L., 2007. Retinal abnormalities in early Alzheimer's disease. *Investigative ophthalmology & visual science,* **48**(5), pp. 2285-2289.

BLANKS, J.C., TORIGOE, Y., HINTON, D.R. and BLANKS, R.H., 1996. Retinal pathology in Alzheimer's disease. I. Ganglion cell loss in foveal/parafoveal retina. *Neurobiology of aging,* **17**(3), pp. 377-384.

CHRISTEN, Y., 2000. Oxidative stress and Alzheimer disease. *The American Journal of Clinical Nutrition,* **71**(2), pp. 621S-629S.

CUMMINGS, B.J., MASON, A.J., KIM, R.C., SHEU, P.C. and ANDERSON, A.J., 2002. Optimization of techniques for the maximal detection and quantification of Alzheimer's-related neuropathology with digital imaging. *Neurobiology of aging,* **23**(2), pp. 161-170.

D'ANDREA, M.R., REISER, P.A., POLKOVITCH, D.A., GUMULA, N.A., BRANCHIDE, B., HERTZOG, B.M., SCHMIDHEISER, D., BELKOWSKI, S., GASTARD, M.C. and ANDRADE-GORDON, P., 2003. The use of formic acid to embellish amyloid plaque detection in Alzheimer's disease tissues misguides key observations. *Neuroscience letters,* **342**(1-2), pp. 114-118.

DE LA TORRE, J.C., 2002. Alzheimer disease as a vascular disorder: nosological evidence. *Stroke,* **33**(4), pp. 1152-1162.

DE LA TORRE, J.C., 2004. Is Alzheimer's disease a neurodegenerative or a vascular disorder? Data, dogma, and dialectics. *The Lancet.Neurology,* **3**(3), pp. 184-190.

DOUBLE, K.L., HALLIDAY, G.M., KRIL, J.J., HARASTY, J.A., CULLEN, K., BROOKS, W.S., CREASEY, H. and BROE, G.A., 1996. Topography of brain atrophy during normal aging and Alzheimer's disease. *Neurobiology of aging,* **17**(4), pp. 513-521.

DUTESCU, R.M., LI, Q.X., CROWSTON, J., MASTERS, C.L., BAIRD, P.N. and CULVENOR, J.G., 2009. Amyloid precursor protein processing and retinal pathology in mouse models of Alzheimer's disease. *Graefe's archive for clinical and experimental ophthalmology = Albrecht von Graefes Archiv fur klinische und experimentelle Ophthalmologie,* **247**(9), pp. 1213-1221.

ETCHEVERS, H.C., VINCENT, C., LE DOUARIN, N.M. and COULY, G.F., 2001. The cephalic neural crest provides pericytes and smooth muscle cells to all blood vessels of the face and forebrain. *Development (Cambridge, England),* **128**(7), pp. 1059-1068.

FERREIRA, D., PERESTELO-PEREZ, L., WESTMAN, E., WAHLUND, L.O., SARRIA, A. and SERRANO-AGUILAR, P., 2014. Meta-Review of CSF Core Biomarkers in Alzheimer's Disease: The State-of-the-Art after the New Revised Diagnostic Criteria. *Frontiers in aging neuroscience,* **6**, pp. 47.

FRAUTSCHY, S.A., YANG, F., IRRIZARRY, M., HYMAN, B., SAIDO, T.C., HSIAO, K. and COLE, G.M., 1998. Microglial response to amyloid plaques in APPsw transgenic mice. *The American journal of pathology,* **152**(1), pp. 307-317.

FROST, S., KANAGASINGAM, Y., SOHRABI, H., VIGNARAJAN, J., BOURGEAT, P., SALVADO, O., VILLEMAGNE, V., ROWE, C.C., MACAULAY, S.L., SZOEKE, C., ELLIS, K.A., AMES, D., MASTERS, C.L., RAINEY-SMITH, S., MARTINS, R.N. and AIBL RESEARCH, G., 2013. Retinal vascular biomarkers for early detection and monitoring of Alzheimer's disease. *Translational psychiatry,* **3**, pp. e233.

GARCIA-ALLOZA, M., BORRELLI, L.A., ROZKALNE, A., HYMAN, B.T. and BACSKAI, B.J., 2007. Curcumin labels amyloid pathology in vivo, disrupts existing plaques, and partially restores distorted neurites in an Alzheimer mouse model. *Journal of neurochemistry,* **102**(4), pp. 1095-1104.

GARCIA-ALLOZA, M., GREGORY, J., KUCHIBHOTLA, K.V., FINE, S., WEI, Y., AYATA, C., FROSCH, M.P., GREENBERG, S.M. and BACSKAI, B.J., 2011. Cerebrovascular lesions induce transient beta-amyloid deposition. *Brain: a journal of neurology,* **134**(Pt 12), pp. 3697-3707.

GOLDSTEIN, L.E., MUFFAT, J.A., CHERNY, R.A., MOIR, R.D., ERICSSON, M.H., HUANG, X., MAVROS, C., COCCIA, J.A., FAGET, K.Y., FITCH, K.A., MASTERS, C.L., TANZI, R.E., CHYLACK, L.T.,JR and BUSH, A.I., 2003. Cytosolic beta-amyloid deposition and supranuclear cataracts in lenses from people with Alzheimer's disease. *Lancet (London, England),* **361**(9365), pp. 1258-1265.

GOTZ, J., CHEN, F., VAN DORPE, J. and NITSCH, R.M., 2001. Formation of neurofibrillary tangles in P301l tau transgenic mice induced by Abeta 42 fibrils. *Science (New York, N.Y.),* **293**(5534), pp. 1491-1495.

GOTZ, J. and ITTNER, L.M., 2008. Animal models of Alzheimer's disease and frontotemporal dementia. *Nature reviews.Neuroscience,* **9**(7), pp. 532-544.

GRUNDKE-IQBAL, I., IQBAL, K., TUNG, Y.C., QUINLAN, M., WISNIEWSKI, H.M. and BINDER, L.I., 1986. Abnormal phosphorylation of the microtubule-associated protein tau (tau) in Alzheimer cytoskeletal pathology. *Proceedings of the National Academy of Sciences of the United States of America,* **83**(13), pp. 4913-4917.

GUPTA, V.K., CHITRANSHI, N., GUPTA, V.B., GOLZAN, M., DHEER, Y., WALL, R.V., GEORGEVSKY, D., KING, A.E., VICKERS, J.C., CHUNG, R. and GRAHAM, S., 2016. Amyloid beta accumulation and inner retinal degenerative changes in Alzheimer's disease transgenic mouse. *Neuroscience letters,* **623**, pp. 52-56.

HARDY, J.A. and HIGGINS, G.A., 1992. Alzheimer's disease: the amyloid cascade hypothesis. *Science (New York, N.Y.),* **256**(5054), pp. 184-185.

HARDY, J. and SELKOE, D.J., 2002. The amyloid hypothesis of Alzheimer's disease: progress and problems on the road to therapeutics. *Science (New York, N.Y.),* **297**(5580), pp. 353-356.

HO, C.Y., TRONCOSO, J.C., KNOX, D., STARK, W. and EBERHART, C.G., 2014. Beta-amyloid, phospho-tau and alpha-synuclein deposits similar to those in the brain are not identified in the eyes of Alzheimer's and Parkinson's disease patients. *Brain pathology (Zurich, Switzerland),* **24**(1), pp. 25-32.

IADECOLA, C., 2010. The overlap between neurodegenerative and vascular factors in the pathogenesis of dementia. *Acta Neuropathologica,* **120**(3), pp. 287-296.

JAVAID, F.Z., BRENTON, J., GUO, L. and CORDEIRO, M.F., 2016. Visual and Ocular Manifestations of Alzheimer's Disease and Their Use as Biomarkers for Diagnosis and Progression. *Frontiers in neurology,* **7**, pp. 55.

JOHNSON, K.A., FOX, N.C., SPERLING, R.A. and KLUNK, W.E., 2012. Brain imaging in Alzheimer disease. *Cold Spring Harbor perspectives in medicine,* **2**(4), pp. a006213.

JOHNSON, L.V., LEITNER, W.P., RIVEST, A.J., STAPLES, M.K., RADEKE, M.J. and ANDERSON, D.H., 2002. The Alzheimer's Abeta-peptide is deposited at sites of complement activation in pathologic deposits associated with aging and age-related macular degeneration. *Proceedings of the National Academy of Sciences of the United States of America,* **99**(18), pp. 11830-11835.

JOHNSON, L.V., LEITNER, W.P., STAPLES, M.K. and ANDERSON, D.H., 2001. Complement activation and inflammatory processes in Drusen formation and age related macular degeneration. *Experimental eye research,* **73**(6), pp. 887-896.

JOHNSON, L.V., OZAKI, S., STAPLES, M.K., ERICKSON, P.A. and ANDERSON, D.H., 2000. A potential role for immune complex pathogenesis in drusen formation. *Experimental eye research,* **70**(4), pp. 441-449.

KAYED, R., HEAD, E., THOMPSON, J.L., MCINTIRE, T.M., MILTON, S.C., COTMAN, C.W. and GLABE, C.G., 2003. Common structure of soluble amyloid oligomers implies common mechanism of pathogenesis. *Science (New York, N.Y.),* **300**(5618), pp. 486-489.

KOIKE, M.A., GREEN, K.N., BLURTON-JONES, M. and LAFERLA, F.M., 2010. Oligemic hypoperfusion differentially affects tau and amyloid-{beta}. *The American journal of pathology,* **177**(1), pp. 300-310.

KORONYO, Y., BIGGS, D., BARRON, E., BOYER, D.S., PEARLMAN, J.A., AU, W.J., KILE, S.J., BLANCO, A., FUCHS, D.T., ASHFAQ, A., FRAUTSCHY, S., COLE, G.M., MILLER, C.A., HINTON, D.R., VERDOONER, S.R., BLACK, K.L. and KORONYO-HAMAOUI, M., 2017. Retinal amyloid pathology and proof-of-concept imaging trial in Alzheimer's disease. *JCI insight,* **2**(16), pp. 10.1172/jci.insight.93621.

KORONYO-HAMAOUI, M., KORONYO, Y., LJUBIMOV, A.V., MILLER, C.A., KO, M.K., BLACK, K.L., SCHWARTZ, M. and FARKAS, D.L., 2011. Identification of amyloid plaques in retinas from Alzheimer's patients and noninvasive in vivo optical imaging of retinal plaques in a mouse model. *NeuroImage,* **54 Suppl 1**, pp. S204-17.

KOYAMA, A., OKEREKE, O.I., YANG, T., BLACKER, D., SELKOE, D.J. and GRODSTEIN, F., 2012. Plasma amyloid-beta as a predictor of dementia and cognitive decline: a systematic review and meta-analysis. *Archives of Neurology,* **69**(7), pp. 824-831.

LAFERLA, F.M., GREEN, K.N. and ODDO, S., 2007. Intracellular amyloid-beta in Alzheimer's disease. *Nature reviews.Neuroscience,* **8**(7), pp. 499-509.

LA MORGIA, C., ROSS-CISNEROS, F.N., KORONYO, Y., HANNIBAL, J., GALLASSI, R., CANTALUPO, G., SAMBATI, L., PAN, B.X., TOZER, K.R., BARBONI, P., PROVINI, F., AVANZINI, P., CARBONELLI, M., PELOSI, A., CHUI, H., LIGUORI, R., BARUZZI, A., KORONYO-HAMAOUI, M., SADUN, A.A. and CARELLI, V., 2016. Melanopsin retinal ganglion cell loss in Alzheimer disease. *Annals of Neurology,* **79**(1), pp. 90-109.

LIM, J.K., LI, Q.X., HE, Z., VINGRYS, A.J., WONG, V.H., CURRIER, N., MULLEN, J., BUI, B.V. and NGUYEN, C.T., 2016. The Eye As a Biomarker for Alzheimer's Disease. *Frontiers in neuroscience,* **10**, pp. 536.

LIU, B., RASOOL, S., YANG, Z., GLABE, C.G., SCHREIBER, S.S., GE, J. and TAN, Z., 2009. Amyloid-peptide vaccinations reduce {beta}-amyloid plaques but exacerbate vascular deposition and inflammation in the retina of Alzheimer's transgenic mice. *The American journal of pathology,* **175**(5), pp. 2099-2110.

LOFFLER, K.U., EDWARD, D.P. and TSO, M.O., 1995. Immunoreactivity against tau, amyloid precursor protein, and beta-amyloid in the human retina. *Investigative ophthalmology & visual science,* **36**(1), pp. 24-31.

LUCHSINGER, J.A., REITZ, C., HONIG, L.S., TANG, M.X., SHEA, S. and MAYEUX, R., 2005. Aggregation of vascular risk factors and risk of incident Alzheimer disease. *Neurology,* **65**(4), pp. 545-551.

LUIBL, V., ISAS, J.M., KAYED, R., GLABE, C.G., LANGEN, R. and CHEN, J., 2006. Drusen deposits associated with aging and age-related macular degeneration contain nonfibrillar amyloid oligomers. *The Journal of clinical investigation,* **116**(2), pp. 378-385.

MANCZAK, M., ANEKONDA, T.S., HENSON, E., PARK, B.S., QUINN, J. and REDDY, P.H., 2006. Mitochondria are a direct site of Abeta accumulation in Alzheimer's disease neurons: implications for free radical generation and oxidative damage in disease progression. *Human molecular genetics,* **15**(9), pp. 1437-1449.

MASTERS, C.L., SIMMS, G., WEINMAN, N.A., MULTHAUP, G., MCDONALD, B.L. and BEYREUTHER, K., 1985. Amyloid plaque core protein in Alzheimer disease and Down syndrome. *Proceedings of the National Academy of Sciences of the United States of America,* **82**(12), pp. 4245-4249.

MCKHANN, G.M., KNOPMAN, D.S., CHERTKOW, H., HYMAN, B.T., JACK, C.R.,JR, KAWAS, C.H., KLUNK, W.E., KOROSHETZ, W.J., MANLY, J.J., MAYEUX, R., MOHS, R.C., MORRIS, J.C., ROSSOR, M.N., SCHELTENS, P., CARRILLO, M.C., THIES, B., WEINTRAUB, S. and PHELPS, C.H., 2011. The diagnosis of dementia due to Alzheimer's disease: recommendations from the National Institute on Aging-Alzheimer's Association workgroups on diagnostic guidelines for Alzheimer's disease. *Alzheimer's & dementia: the journal of the Alzheimer's Association,* **7**(3), pp. 263-269.

MULLINS, R.F., RUSSELL, S.R., ANDERSON, D.H. and HAGEMAN, G.S., 2000. Drusen associated with aging and age-related macular degeneration contain proteins common to extracellular deposits associated with atherosclerosis, elastosis, amyloidosis, and dense deposit disease. *FASEB journal: official publication of the Federation of American Societies for Experimental Biology,* **14**(7), pp. 835-846.

NING, A., CUI, J., TO, E., ASHE, K.H. and MATSUBARA, J., 2008. Amyloid-beta deposits lead to retinal degeneration in a mouse model of Alzheimer disease. *Investigative ophthalmology & visual science,* **49**(11), pp. 5136-5143.

ODDO, S., CACCAMO, A., SMITH, I.F., GREEN, K.N. and LAFERLA, F.M., 2006. A dynamic relationship between intracellular and extracellular pools of Abeta. *The American journal of pathology,* **168**(1), pp. 184-194.

OHYAGI, Y., TSURUTA, Y., MOTOMURA, K., MIYOSHI, K., KIKUCHI, H., IWAKI, T., TANIWAKI, T. and KIRA, J., 2007. Intraneuronal amyloid beta42 enhanced by heating but counteracted by formic acid. *Journal of neuroscience methods,* **159**(1), pp. 134-138.

PADURARIU, M., CIOBICA, A., MAVROUDIS, I., FOTIOU, D. and BALOYANNIS, S., 2012. Hippocampal neuronal loss in the CA1 and CA3 areas of Alzheimer's disease patients. *Psychiatria Danubina,* **24**(2), pp. 152-158.

PATTON, N., ASLAM, T., MACGILLIVRAY, T., PATTIE, A., DEARY, I.J. and DHILLON, B., 2005. Retinal vascular image analysis as a potential screening tool for cerebrovascular disease: a rationale based on homology between cerebral and retinal microvasculatures. *Journal of anatomy,* **206**(4), pp. 319-348.

PENSALFINI, A., ALBAY, R.,3RD, RASOOL, S., WU, J.W., HATAMI, A., ARAI, H., MARGOL, L., MILTON, S., POON, W.W., CORRADA, M.M., KAWAS, C.H. and GLABE, C.G., 2014. Intracellular amyloid and the neuronal origin of Alzheimer neuritic plaques. *Neurobiology of disease,* **71**, pp. 53-61.

PEREZ, S.E., LUMAYAG, S., KOVACS, B., MUFSON, E.J. and XU, S., 2009. Beta-amyloid deposition and functional impairment in the retina of the APPswe/PS1DeltaE9 transgenic mouse model of Alzheimer's disease. *Investigative ophthalmology & visual science,* **50**(2), pp. 793-800.

PRICE, J.L., MCKEEL, D.W.,JR, BUCKLES, V.D., ROE, C.M., XIONG, C., GRUNDMAN, M., HANSEN, L.A., PETERSEN, R.C., PARISI, J.E., DICKSON, D.W., SMITH, C.D., DAVIS, D.G., SCHMITT, F.A., MARKESBERY, W.R., KAYE, J., KURLAN, R., HULETTE, C., KURLAND, B.F., HIGDON, R., KUKULL, W. and MORRIS, J.C., 2009. Neuropathology of nondemented aging: presumptive evidence for preclinical Alzheimer disease. *Neurobiology of aging,* **30**(7), pp. 1026-1036.

PRINCE, M., COMAS-HERRERA, A., KNAPP, M., GUERCHET, M. and KARAGIANNIDOU, M., 2016. World Alzheimer Report 2016, Alzheimer's Disease International.

RITCHIE, C.W., PETO, T., BARZEGAR-BEFROEI, N., CSUTAK, A., NDHLOVA, P., WILSON, D., CORRIDAN, B., GOUD, B., CHEESMAN, N. AND LENGYEL, I., 2011. Peripheral Retinal Drusen as a Potential Surrogate Marker for Alzheimer's Dementia: A Pilot Ultra-Wide Angle Imaging Study. *Investigative Ophthalmology and Visual Science*; 52(14) pp.2–11 E-Abstract 6683.

SCHEFF, S.W., PRICE, D.A., SCHMITT, F.A. and MUFSON, E.J., 2006. Hippocampal synaptic loss in early Alzheimer's disease and mild cognitive impairment. *Neurobiology of aging,* **27**(10), pp. 1372-1384.

SCHON, C., HOFFMANN, N.A., OCHS, S.M., BURGOLD, S., FILSER, S., STEINBACH, S., SEELIGER, M.W., ARZBERGER, T., GOEDERT, M., KRETZSCHMAR, H.A., SCHMIDT, B. and HERMS, J., 2012. Long-term in vivo imaging of fibrillar tau in the retina of P301S transgenic mice. *PloS one,* **7**(12), pp. e53547.

SELKOE, D.J., 2001. Alzheimer's disease: genes, proteins, and therapy. *Physiological Reviews,* **81**(2), pp. 741-766.

SELKOE, D.J., 2002. Alzheimer's disease is a synaptic failure. *Science (New York, N.Y.),* **298**(5594), pp. 789-791.

SERRANO-POZO, A., FROSCH, M.P., MASLIAH, E. and HYMAN, B.T., 2011. Neuropathological alterations in Alzheimer disease. *Cold Spring Harbor perspectives in medicine,* **1**(1), pp. a006189.

TARAWNEH, R. and HOLTZMAN, D.M., 2012. The clinical problem of symptomatic Alzheimer disease and mild cognitive impairment. *Cold Spring Harbor perspectives in medicine,* **2**(5), pp. a006148.

THAL, D.R., GRIFFIN, W.S., DE VOS, R.A. and GHEBREMEDHIN, E., 2008. Cerebral amyloid angiopathy and its relationship to Alzheimer's disease. *Acta Neuropathologica,* **115**(6), pp. 599-609.

THE RETINA REFERENCE, 2017-last update, *Normal Retinal Anatomy - The Retina Reference*. [Online]. Available: http://www.retinareference.com/anatomy/2017 [Accessed 14 Aug. 2017].

THOMPSON, R.B., REFFATTO, V., BUNDY, J.G., KORTVELY, E., FLINN, J.M., LANZIROTTI, A., JONES, E.A., MCPHAIL, D.S., FEARN, S., BOLDT, K., UEFFING, M., RATU, S.G., PAULEIKHOFF, L., BIRD, A.C. and LENGYEL, I., 2015. Identification of hydroxyapatite spherules provides new insight into subretinal pigment epithelial deposit formation in the aging eye. *Proceedings of the National Academy of Sciences of the United States of America,* **112**(5), pp. 1565-1570.

TSAI, Y., LU, B., LJUBIMOV, A.V., GIRMAN, S., ROSS-CISNEROS, F.N., SADUN, A.A., SVENDSEN, C.N., COHEN, R.M. and WANG, S., 2014. Ocular changes in TgF344-AD rat model of Alzheimer's disease. *Investigative ophthalmology & visual science,* **55**(1), pp. 523-534.

WANG, L., CLARK, M.E., CROSSMAN, D.K., KOJIMA, K., MESSINGER, J.D., MOBLEY, J.A. and CURCIO, C.A., 2010. Abundant lipid and protein components of drusen. *PloS one,* **5**(4), pp. e10329.

WILLIAMS, M.A., MCGOWAN, A.J., CARDWELL, C.R., CHEUNG, C.Y., CRAIG, D., PASSMORE, P., SILVESTRI, G., MAXWELL, A.P. and MCKAY, G.J., 2015. Retinal microvascular network attenuation in Alzheimer's disease. *Alzheimer's & dementia (Amsterdam, Netherlands),* **1**(2), pp. 229-235.

YANKNER, B.A., 1996. Mechanisms of neuronal degeneration in Alzheimer's disease. *Neuron,* **16**(5), pp. 921-932.

YASOJIMA, K., SCHWAB, C., MCGEER, E.G. and MCGEER, P.L., 1999. Up-regulated production and activation of the complement system in Alzheimer's disease brain. *The American journal of pathology,* **154**(3), pp. 927-936.

ZHAO, J., DENG, Y., JIANG, Z. and QING, H., 2016. G Protein-Coupled Receptors (GPCRs) in Alzheimer's Disease: A Focus on BACE1 Related GPCRs. *Frontiers in aging neuroscience,* **8**, pp. 58.

ZLOKOVIC, B.V., 2011. Neurovascular pathways to neurodegeneration in Alzheimer's disease and other disorders. *Nature reviews.Neuroscience,* **12**(12), pp. 723-738.